Morphostructural evidence of Late Quaternary tectonics at the Po Plain-Northern Apennines border (Lombardy, Italy)

Chiara Zuffetti, Riccardo Bersezio

PII: S0169-555X(20)30217-8

DOI: https://doi.org/10.1016/j.geomorph.2020.107245

Reference: GEOMOR 107245

To appear in: *Geomorphology*

Received date: 26 December 2019

Revised date: 11 May 2020

Accepted date: 11 May 2020

Please cite this article as: C. Zuffetti and R. Bersezio, Morphostructural evidence of Late Quaternary tectonics at the Po Plain-Northern Apennines border (Lombardy, Italy), *Geomorphology* (2020), https://doi.org/10.1016/j.geomorph.2020.107245

Highlights

1. Palimpsest landscapes mirror polyphase tectonic evolution of foreland basins
2. Effects of locked, blind thrust-and-fold belts on surface processes and landforms
3. Field-based case-history on morphotectonics of the Quaternary Po Foreland Basin
4. Late Pleistocene growth, segmentation and collapse of intrabasinal highs
5. Neotectonics and seismicity control the river network of basins and highs

Graphical Abstract

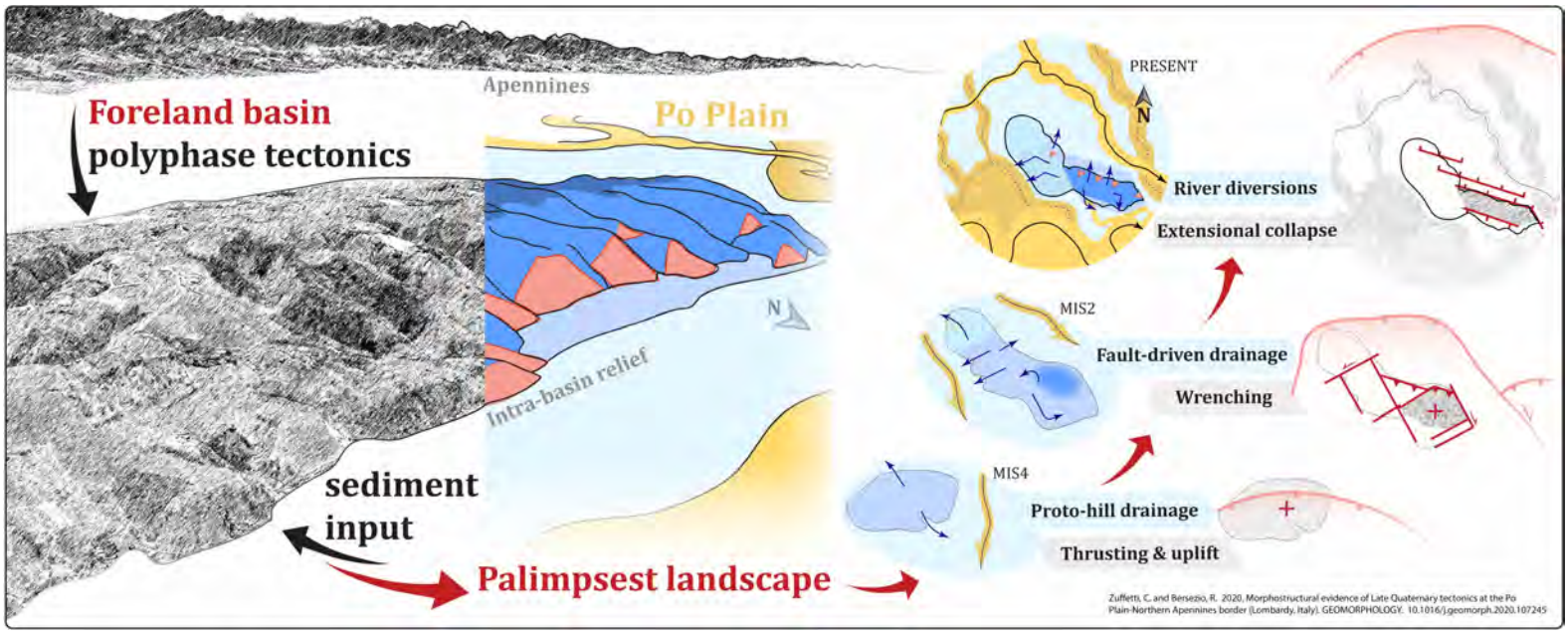

C. Zuffetti and R. Bersezio, Morphostructural evidence of Late Quaternary tectonics at the Po Plain-Northern Apennines border (Lombardy, Italy), Geomorphology (2020), https://doi.org/10.1016/j.geomorph.2020.107245

Morphostructural evidence of Late Quaternary tectonics at the Po Plain-Northern Apennines border (Lombardy, Italy)

Chiara Zuffetti*, Riccardo Bersezio

Dipartimento di Scienze della Terra, Università degli Studi di Milano, via Mangiagalli 34, 20133 I-Milano, Italy

**Corresponding Author. Authors e-mail: Chiara Zuffetti:* chiara.zuffetti@unimi.it *(OrcID 0000-0002-7391-4829); Riccardo Bersezio:* riccardo.bersezio@unimi.it *(OrcID 0000-0002-6629-8917).*

ABSTRACT The landscape of foreland basins adjacent to active mountain ranges evolves under the control of basinward tectonic propagation of the structural fronts, in competition with climate dynamics. The resulting palimpsest landscapes record the sequence of geomorphic evolutionary steps, and the spatial-temporal relations between the active geological processes. However, a precise evolutionary sequence is hard to decipher from low-relief settings, like the wide alluvial plains worldwide. About these topics we investigate the sequence of tectonic- and climate-driven processes which shaped the palimpsest landscape of a large Quaternary foreland basin, the Po Plain in Northern Italy. Above the average glacio-fluvial and alluvial plain of the basin, Late Quaternary intra-basin reliefs emerge, owing to syndepositional ramp folding and uplift driven by N-wards propagation of the outermost thrust fronts of the active N-Apennine chain.

The incremental tectono-morphological and depositional history of the region permits to describe the propagation of the structural front as a polyphase process, involving uplift, wrenching and late collapse of the reliefs. This history is documented by: relicts of uplifted planation surfaces covered by latest Pleistocene weathered loess units; polygonal facets, landslides and slope wedges along faults delineating the slopes of the largest among the intra-basin reliefs (San Colombano hill); hydrographic anomalies on the relief network (river diversions, piracy and perching of valleys, paleovalley fills), river diversions and cross-cut relations on the adjacent alluvial plain. These features testify the thrust-fold-related, pre-LGM uplift of the Late Pleistocene alluvial stratigraphy, the subsequent segmentation of the relief in differently uplifting blocks along Riedel faults, owing to activation of a transfer fault zone, and the LGM extensional collapse of the relief, along inherited fault systems. A late, post-glacial outwards propagation of the Apennine thrusts was buttressed by the opponent Alpine thrust-belt front and induced the entrenchment of the river network. River diversions on the plain were controlled by the orientation of the San Colombano hill fault systems. The distribution of historical earthquakes and the present-day geodetic data are coherent with this evolution.

The study documents how, in foreland basins, the syndepositional propagation of "blind" orogenic fronts shapes the palimpsest landscape with superimposed morphological, tectonic, and stratigraphic features of paleoseismic significance, and permits comparisons with the other low-relief basin settings worldwide.

Keywords: foreland basin; northern Apennines; Po Plain; Quaternary

1. Introduction

Complex palimpsest landscapes (Bloom, 2002) represent important archives of the geological evolution of

sedimentary basins and mountain ranges. In Quaternary continental foreland basins facing active thrust belts, the outwards propagation of the structural fronts from the main range, controls the polyphase evolution of basin landscapes. Buried thrusts, fault-propagation-folds, and transfer zones propagate inside the basins, inducing the outward-shift of depocenters and structural highs (Morley, 1986; Ricci Lucchi, 1986; Butler, 1987; Dunne and Ferill, 1988; Morley, 1988; McClay, 1992), restyling the landscape features at each tectonic increment. In these settings, polyphase faulting conditions landscape evolution competing with climate-driven dynamics (Keller and Pinter, 2002; Burbank and Anderson, 2013). When the main landscape-shaping tectonic structures are blind or buried below the topographic surface, the evidence and relative chronology of their activity may be deduced by combining geomorphological and geological field-based investigations, and help to refine the regional models of basin evolution (Holbrook and Schumm, 1999; Schumm et al., 2002; Burrato et al., 2003). Geomorphological features also witness the tectonic deformation in low-relief basin settings, like the wide Quaternary alluvial plains of the world. In these cases, the pattern of the hydrographic network, conditioned by changes of the topographic gradient, marks the landscape modifications linked to recent/active tectonics (examples in Schumm et al., 2002; Burrato et al., 2003; Zámolyi et al., 2010).

Among the foreland basins of the world, the Quaternary Po Basin (N-Italy; Fig.1-A) represents a good case-history to present insights on the geomorphological implications of tectonics on palimpsest landscape evolution of a typical low-relief alluvial plain basin setting. The Po alluvial plain elongates WNW-to-ESE between the opposite fronts of two mountain ranges, the Southern Alps to the North and the Northern Apennines to the South. Since the Late Miocene, this region represents the foreland of the active N-Apennines fold-and-thrust belt, whose salients propagated N- and NE-wards, cross-cutting the buried frontal thrusts of the Southern Alps (Fig.1-A), and controlling subsidence-sedimentation patterns (Pieri and Groppi, 1981; Bigi et al., 1990; Doglioni, 1993; Carminati et al., 2003; Fantoni et al., 2004). The interference between the two chains contributed to buttress the foreland propagation of the Apennines thrusts, which is the peculiar feature of the central Po Plain foreland, differently from its eastern prolongation towards the Adriatic foredeep (Castiglioni and Pellegrini, 2001; Ghielmi et al., 2013). A set of Quaternary intra-basin reliefs emerges above the average elevation of the alluvial plain (Desio, 1965; Fig.1-A), over the culminations of the deep ramp folds of both the thrust belts. Recent studies described the evidence of the Quaternary morphotectonic evolution of these intra-basin reliefs, by integrating geomorphological analyses and field-based stratigraphic, geopedological and structural analyses (Benedetti et al., 2003; Pellegrini et al., 2003; Bresciani and Perotti, 2014; Livio et al., 2014; Zuffetti et al. 2018a, 2018b). However, the immediate effect of foreland propagation of the Apennines thrust system on the polyphase landscape evolution, and a full

comprehension of the coevolution of these intra-basin reliefs, has not yet been resolved in the available literature.

Here we contribute to understand the relationships between the geomorphic and tectono-sedimentary processes which act in a Quaternary foreland basin, pinched in-between two active fold-and-thrust belts, in a periglacial setting. The addressed questions are: how to detect the relative chronology of the Quaternary morpho-tectonic increments, in peculiar kinds of foreland basins like the Po Basin? How do the coupled palimpsest landforms of the intra-basin reliefs and adjacent alluvial plains preserve the record of this incremental evolution? Do they provide clues to interpret the recent seismicity? Based on a multidisciplinary approach, the paper focuses on the area of the southernmost, widest and highest among the isolated reliefs, the San Colombano Hill at the Apennines side of the basin (Fig.1). It represents the surface geomorphic expression of the San Colombano Hill Structure (SCS[1], Fig.1-A; Desio, 1965; Benedetti et al., 2003; Zuffetti et al., 2018a), a ramp fold of the buried Apennines front. The SCS holds some relevance to understand the tectonic evolution of landscape in foreland basins because: i) its pedo-stratigraphic history records a polyphase evolution, driven by competing Late Quaternary folding, uplift, faulting and climate changes in a periglacial setting (Zuffetti et al., 2018a, 2018b); ii) it sets at the Po Plain-Apennines orogen hinge, where the chronology of the Quaternary morpho-tectonic increments, and the related seismic potential, have not been fully solved in literature (Benedetti et al., 2003; Toscani et al., 2006; Devoti et al., 2011; Ghielmi et al., 2013; Valensise et al., 2020); iii) it permits to study in detail on a local scale effects of basin-scale foreland thrust-propagation folding on landscape evolution, documenting the geomorphic evidence of Late Quaternary faulting associated to uplift and collapse of an intra-basin relief.

[1] Some abbreviations recur in the text. In order to facilitate the reading, the complete list of abbreviations is disclosed here, in alphabetical order. CPPS: Central Po Plain Structures; CPS1: Cascina Parina 1 Synthem; CPS2: Cascina Parina 2 Synthem; CZTF: Casalpusterlengo-Zorlesco Transfer Fault; CZS: Casalpusterlengo-Zorlesco Structure; INS: Invernino Synthem; L: LGM loess cover; LGM: Last Glacial Maximum; MLS: Monteleone Synthem; PCLR: Pavia-Casteggio Lateral Ramp; PML: Po Plain Main Level; POS: Po Synthem; SCS: San Colombano Structure.

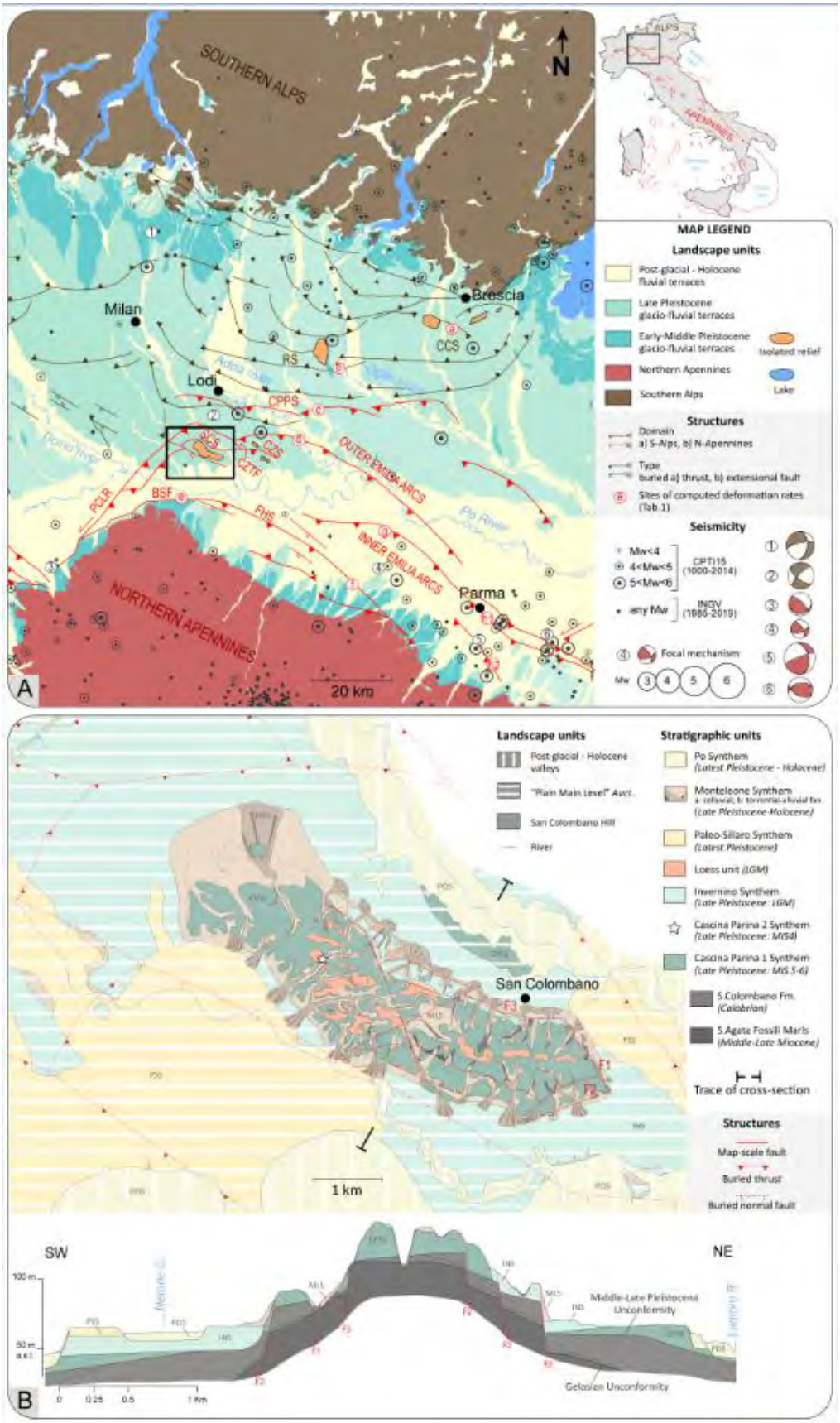

Fig. 1 – A) Location map of the study area in the structural and seismic framework of the Po Plain (Northern Italy). The study area (black frame) hosts the southernmost of a set of intra-basin isolated reliefs. Buried S-Alpine structures simplified from Fantoni et al. (2004). Buried N-Apennines structures from Bigi et al. (1990). Location of historical earthquakes after INGV (http://cnt.rm.ingv.it); Rovida et al. (2016). Earthquakes focal mechanisms from EMMA (Earthquake Mechanisms of the

Mediterranean Area; Vannucci and Gasperini, 2004) catalog and RCMT (European-Mediterranean Regional Centroid Moment Tensor; Pondrelli et al, 2002) catalog of INGV. CCS: Capriano del Colle Structure, CPPS: Central Po Plain Structures, RS: Romanengo structure, SCS: San Colombano hill Structure, CZS: Casalpusterlengo-Zorlesco Structure, CZTF: Casalpusterlengo-Zorlesco Transfer Fault, BSF: Broni-Stradella Fault, FHS: Foothill Structures. B) Stratigraphic and landscape units of the San Colombano hill study area (location in panel A). F1-F3: interpreted map-scale fault systems, orientations: N160E (F1); N060E (F2); N110E (F3). Modified after Zuffetti et al. (2018a).

ID (Fig. 1-A)	Fault system (Fig. 1-A)	Age interval	Slip rate [mm/yr]	Slip rate type	Uplift rate [mm/yr]	Authors
a	CCS	0.8 My-present	0.47	DSR	0.22	Livio et al. (2009)
b	RS	Late Pleistocene-present			0.12	Bresciani and Perotti (2014)
c	CPPS	1.8 My-present	0.19	DSR		Maesano et al. (2015)
d	Outer Emilia Arcs	1.8 My-present	0.51	DSR		Maesano et al. (2015)
	Outer Emilia Arcs	1.8 My-present	1.5	RSR		Boccaletti et al. (2011)
e	BSF	Late Pleistocene-present			0.3	Benedetti et al. (2003)
f	FHS	0.8 My-present	0.5	DSR	0.1-0.3	Wilson et al. (2009)
g	Inner Emilia Arcs	0.8 My-present	0.22	DSR		Maesano et al. (2015)
h1	Inner Emilia Arcs	0.8 My-present	0.26	DSR		Maesano et al. (2015)
h2	Inner Emilia Arcs	0.8 My-present	0.3	DSR		Maesano et al. (2015)

Table 1 – Slip rates and uplift rate ranges along the South Alpine and Northern Apennines thrusts in the Central Po foreland basin. DSR/RSR: dip parallel/rake parallel slip rates.

2. The San Colombano Hill Structure: geological setting of the Po Basin-Northern Apennines hinge

The SCS (Fig.1-A) belongs to the N115E-striking, outer fronts of the Emilia Arc, a set of buried structural arcs of the N-Apennines which have been progressively migrating N-wards since the Late Miocene, along the N035E-striking Pavia-Casteggio lateral ramp (PCLR, Fig.1-A; Benedetti et al., 2003). East of the SCS, the outer Emilia Arcs comprise the Casalpusterlengo-Zorlesco buried structures, associated to the homonymous subtle topographic reliefs (CZS, Fig.1; Desio, 1965; Ariati et al., 1988; Zuffetti et al., 2018b). The outermost Apennine Arcs intersect the opposite verging front of Southern Alps, along a buried W-E belt just North of the study area (CPPS, Fig.1-A). The neotectonic activity of the Emilia Arcs is claimed by regional geomorphological evidence (e.g. location of isolated reliefs and Holocene river anomalies on ramp anticline culminations) and is supported by paleoseismic and geodetic data (Desio, 1965; Pellegrini and Vercesi, 1995; Burrato et al., 2003; Di Manna et al., 2012; Alessio et al., 2013; Bonini et al., 2014; Maestrelli et al., 2018). Based on these data, rates of N-ward shortening across the central-southern Po Basin range between 0.4 and 1.5 mm/yr (higher values towards the East; Devoti et al., 2011; Bennett et al., 2012; Michetti et al., 2012; Farolfi et al., 2019). Topographic leveling (Arca and Beretta, 1985) identified anomalous uplift trends at the SCS, characterised by positive isokinetics ranging around 0.5 mm/yr, if compared to the general slower trend of the adjacent Po plain.

The Outer Emilia Arcs is one of the main seismogenic sources of N-Italy (DISS Working Group, 2018), for which a cumulative slip rate of 0.7 mm/yr and depths between 2 and 7 km were proposed by Maesano et al. (2015) over the past 1.8 Myr (site d, Fig.1-A; Table1). To the South, Late Quaternary uplift rates of 0.3 mm/yr were inferred for the outcropping Emilia Arcs by Benedetti et al. (2003; BSF, Fig.1-A; Table 1). Historical and instrumental catalogues (Boschi et al., 2000; Guidoboni et al., 2007; Vannoli et al., 2015; Rovida et al., 2016) show a sparse moderate seismicity in the region of the Outer Emilia Arc (4.5<Mw<5.0, Fig.1-A), with the exception of the damaging earthquakes on 28 July 1276 (Mw 5.1, depth<12 km; Rovida et al., 2016), 7 April 1786 (Mw 5.2, depth>15 km; Piovene, 1888; Postpischl, 1985), 15 May 1951 (Mw 5.2, depth>15 km) that hit the Lodi area (nr.2; Fig.1-A), some km North of the SCS, suggesting slip rates on local buried faults. NE of the study area, the 12 May 1802 event (Mw 5.6, depth<12 km) near the Oglio river was related to active slip along the southernmost, buried frontal Southalpine thrust (b, Fig.1-A; Table 1). To the SE, the 11 June 1438 event (Mw 5.6) suggests local shallow activity of the buried Inner Emilia Arcs near Parma (Fig.1-A). Contractional focal mechanisms (Pondrelli, 2002; Vannucci and Gasperini, 2004; Pondrelli et al., 2011) dominate the Inner and eastern Emilia Arcs (3-to-6, Fig.1-A), while strike-slip to oblique-slip mechanisms characterize earthquakes above the CPPS and the Southalpine thrusts to the North (1-2, Fig.1-A). A dominant, active compressional tectonic regime has been also documented by stress orientation data, showing mean directions of Sh_{max} perpendicular to the trend of the buried Emilia Arc fronts (Montone et al., 2012; Carafa and Barba, 2013), and confirming that these structures are favorably oriented with the direction of regional tectonic shortening. Exceptions are the WSW-ENE trends of Sh_{max} in-between the western Outer Emilia Arc and the CPPS, at the same locations where focal mechanisms show dominant strike-slip components (Fig.1-A). Focal solutions and orientation data indicate that the Late Quaternary regional tectonics at the Po Plain-Apennines hinge has been dominated by northward thrusting-and-folding, with local transpression along lateral ramps and at deeper reactivation sites of the Southalpine thrusts (Pieri and Groppi, 1981; Bonini et al., 2014; Bresciani and Perotti, 2014; Livio et al., 2014; Turrini et al., 2015; Livani et al., 2018). Local evidence of Quaternary extensional faulting were instead described by Capozzi et al. (1994), Pellegrini and Vercesi (1995), Bertotti et al. (1997), in the Northern Emilia Apennines, by Zuffetti et al. (2018a) in the study area, and discussed in the NW Apennines by Molli et al. (2018). Quaternary activation of extensional faults in the northern Apennines was also supported by the investigation of natural fluid seeps (Capozzi and Picotti, 2002, 2010; Bonini, 2013). Thermal fluid vents and related diagenetic features underline the main tectonic structures at the Po Plain-Apennines border (Chiarle et al., 1991; Capozzi et al., 1994; Conti et al., 2001, 2007; Oppo et al., 2017). In the SCS area, the location of thermal/mineralized springs and hydrocarbon vents, in close relationships with the

morphotectonic elements, is apparently linked with the disjunctive structures.

2.1 The San Colombano hill

The San Colombano hill elevates of maximum 70 m above the 'Plain Main Level' (Castiglioni and Pellegrini, 2001; PML, Fig.1-B), the widest geomorphological unit of the Po Plain. The eastern hill is characterised by straight steep slopes becoming more gentle westwards, where a gradual transition to the PML occurs. On the hill, three NW-ward down-stepping morphological sectors were mapped by Boni (1967) and Benedetti et al. (2003) and interpreted as relicts of alluvial terraces, abraded during the Late Pleistocene uplift of the SCS. Zuffetti et al. (2018a, 2018b), relying on stratigraphic and geopedological evidence, identified four fault-blocks, originated during Late Pleistocene hill dissection by three fault systems, F1 (N160E), F2 (N060E), F3 (N110E, Fig.1-B). The terraced plain surrounding the hill is crossed by several NNW-SSE-trending abandoned meandering river traces (Veggiani, 1982; Bersezio, 1986; Marchetti, 2002). The present-day river network cross-cuts these traces and is entrenched within the plain since post-glacial times (Fig.1-A).

The Quaternary succession of the study area belongs to a regional, Alpine-sourced regressive sequence developed above the Mio-Pliocene marine substratum (Regione Lombardia and Eni, 2001; Ghielmi et al., 2013). The hill exposes the folded Upper Miocene marine sediments (Boni, 1967; Fig.1-B), which are covered by Lower Pleistocene, shallow-water transgressive sediments (Boni, 1967; Zuffetti et al., 2018a; Gelasian Unconformity; Ghielmi et al., 2013). Only the southern upright and S-dipping backlimb of the pre-Gelasian anticline is preserved, because the N-dipping forelimb is down-faulted North of the hilltop (Fig.1-B-cross-section). During the Early *pro parte*-Middle Pleistocene, the Gelasian Unconformity was folded around a N100E-striking axis and cut by the Middle-Late Pleistocene angular unconformity (Zuffetti et al., 2018a). The age of this composite unconformity is constrained by OSL data (Panzeri et al., 2011), which attribute the oldest alluvial and glacio-fluvial units sitting above it to the MIS5-MIS4 interval (Cascina Parina 1 and 2 Synthems; CPS1 and CPS2, Fig.1-B). We adopted a lithostratigraphic and UBSU classification (NACSN, 2005). The latter applies to units identified by unconformable boundaries physically correlated throughout the area (Chiarini et al., 2008; Zuffetti et al., 2018a). The uplifted CPS1 is covered by weathered MIS4 loess in the western hill (Zuffetti et al., 2018b). On the hill, the subsequent CPS2, correlative to Upper Pleistocene subsurface glacio-fluvial units, is preserved only within relicts of paleo-valleys (Zuffetti, 2019). The pre-Last Glacial Maximum (LGM) synthems are terraced and covered by the LGM glacio-fluvial Invernino Synthem (INS, Fig.1-B), whose age is constrained by radiocarbon age determinations (Baio et al., 2004; Bersezio et al., 2004; Bini et al., 2016; Zuffetti et al., 2018b). Southward-thinning and wedging-out, amalgamation

of bedsets, petrographic changes, and soft-sediment deformations characterize these Late Pleistocene sediments approaching the San Colombano hill, documenting their syntectonic deposition (Zuffetti, 2019; Zuffetti et al., 2018a). A mildly-weathered loess covers CPS1, CPS2 and INS at the hilltop and on flat-top terraces along the northern hillslope (L, Fig.1-B). Widespread colluvial wedges (Monteleone Synthem; MLS, Fig.1-B) blanket the hillslopes. On the surrounding plain, INS and CPS1 are cross-cut by the early post-Glacial Paleo-Sillaro Synthem (PSS) that formed within a shallow terrace run by the mentioned abandoned river traces. The late post-glacial-to-recent entrenchment of the river network led to deposition of the Po Synthem (PoS, Fig.1-B) within the lowermost terraced valleys, cross-cutting PSS. The Late Pleistocene synthems exposed in the study area do not show evidence of folding, while they are affected by local tilting and several meso-scale disjunctive structures. Directions of these structures are coherent with the strike of the straight hillslope segments (Fig.1-B), and are often coupled in conjugate systems (Zuffetti et al., 2018a, 2018b).

3. Methods and techniques

The palimpsest landscape of the San Colombano hill area has been deciphered as sensitive sensor of Late Quaternary tectonic activity, by combining 1:10.000 field geomorphological mapping, field/remote morphotectonic observations and GIS-assisted computations. The new data were integrated with the stratigraphic, sedimentological, pedological and structural data collected during previous works (Zuffetti, 2019; Zuffetti et al., 2018a; b) and literature. Topographic maps, aerial photos, orthophoto (AGEA, 2012) and 5m DTM (www.geoportale.regione.lombardia.it) were also analysed.

3.1 Analysis of the hill front and adjacent plain

The morphological features of hill front segments were surveyed in the field, extracted from DTM and topographic maps. Facet shape and height were measured to examine their changes along the hillslopes. Facet height calculations were obtained by the difference between top and base elevation in GIS. The mountain-front sinuosity index J (Bull, 2007), a classic well-established parameter, was also used to interpret tectonic features in comparison with field observations. J is defined as the ratio of the plan length of the topographic junction between the relief and adjacent piedmont (L_{mf}) vs. the straight-line length of the same front, L_s (Bull, 2007; Bull and Mc Fadden, 1977; Keller and Pinter, 2002; Silva et al., 2003): $J=L_{mf}/L_s$. Values of $1<J<1.4$ suggest highly tectonically-active, straight fronts, whereas $1.4<J<3$ values characterize moderate-to-inactive fronts, dominated by erosional processes. Tectonic tilting of the hill front at the hill-plain junctions was also analysed by evaluating the morphology of alluvial fans along the hillslopes, taking notes from Keller and Pinter (2002).

The surface of the plain adjacent to the hill was analysed by mapping the dip directions of the topographic surface for each agrarian parcel and the nature, height and origin of escarpments (Table 2). The result is a semi-quantitative aspect map of this nearly-flat area, that was compared to the available DTM. This procedure was necessary because the resolution of the DTM does not permit to extract the most gently-dipping landforms.

3.2 Analysis of the drainage network

Drainage network analyses were carried out in GIS and include: nature of drainage patterns/basins, drainage texture, valley shapes, individual stream patterns. The hill drainage network was drawn from field observations, topographic maps and Google Earth® images (SPOT images or products from Digital Globe e.g. Ikonos, QuickBird, with a resolution close to aerial photographs). All the I-IV order streams (Strahler, 1957) were rectified where traceable without relevant changes of direction relative to their length, to compute the azimuth of each segment. Anomalies indicate departures from the regional geological/topographic controls. Rose diagrams permitted comparisons of the directional drainage data with the field measurements of mesofaults and other morphostructural lineaments.

Drainage basin shape (B_s) is defined as the ratio of the length of a drainage basin (B_l) to its maximum width (B_w): $B_s=B_l/B_w$ (Ramírez-Herrera, 1998; El Hamdouni et al., 2008). Long, narrow basins (high Bs values) may be structurally controlled, compared to more circular ones. The asymmetry factor (AF) was used to detect tectonic tilting transverse to the flow of a drainage basin (Cox, 1994; Keller and Pinter, 2002): $AF=100\ (A_r/A_t)$, where A_r is basin area to the right-facing downstream, A_t is the total basin area. Values of AF much lower/higher than 50 may suggest a basin tilting orthogonal to the main trunk stream. These values were discussed as tectonic indicators, after having removed the lithological control on basin development, by integrating geomorphological and geological maps.

Geomorphological datum	GIS element	Geomorphological datum	GIS element
Topographic elevation point	point FC	Geomorphological boundary	polyline FC
Dip-direction of the topographic surface	point FC	Fault	polyline FC
Sub-horizontal agrarian parcel	point FC	Longitudinal profile	polyline FC
Hump; hollow	point FC	Trace of topographic profile	polyline FC
Windgap	point FC	Drainage basin	polygon FC
Saddle	point FC	Planation surface	polygon FC
Back-tilted surface	point FC	Ranked geomorphological unit	polygon FC
Downstream end of hanging valley	point FC	Topographic basemaps	raster dataset
Ranked escarpment (natural; anthropic)	polyline FC	Digital Terrain Model	raster dataset
Rectilinear/cruvilinear tract of the stream network	polyline FC	Digital Surface Model	raster dataset
Drainage divide	polyline FC	Slope and aspect map	raster dataset
Trace of abandoned hydrography	polyline FC	Longitudinal profile graph	raster dataset
Landslide rim	polyline FC	Topographic profile graph	raster dataset
Ridge (tectonic; fluvial)	polyline FC		

FC: GIS Feature Class

Table 2 – The geomorphological dataset and the related GIS elements surveyed and analysed in this work.

3.3 Data management and integration

The geomorphological and structural dataset was digitized and normalized relying on the definition of *ad-hoc* built coded domains. Landforms were grouped in accordance to their genetic attributes, stored in specific GIS Geo-Databases (Table 2), and concurred in defining the morphotectonic setting of the study area. Location of hydrocarbon vents, thermal springs, localized calcium carbonate concretions was also mapped and compared to the distribution of disjunctive features. Rates of displacement were proposed starting from the deformation of (pedo-) stratigraphic and geomorphic markers of known age with respect to the local elevation of those markers, and from the geomorphic features of the hillslopes, taking notes from Bull (2007) and McCalpin (2009).

4. Morphotectonics of the San Colombano hill and surrounding alluvial plains

The hill and adjacent plain display an overall W-E asymmetry in the type and distribution of landscape features. The western, low-relief San Colombano hill (Fig.2) shows rare morphostructures compared to the central-eastern hill and the adjacent northern/southern plain areas. The morphostructural elements are recurrently aligned along the three mentioned orientations (N160E, N060E, N110E, Fig.2). The following sections describe and interpret the features of the western hill area first; these are then compared to the central-eastern hill and adjacent plain morphologies (hilltop, hillslopes, drainage patterns and alluvial landforms).

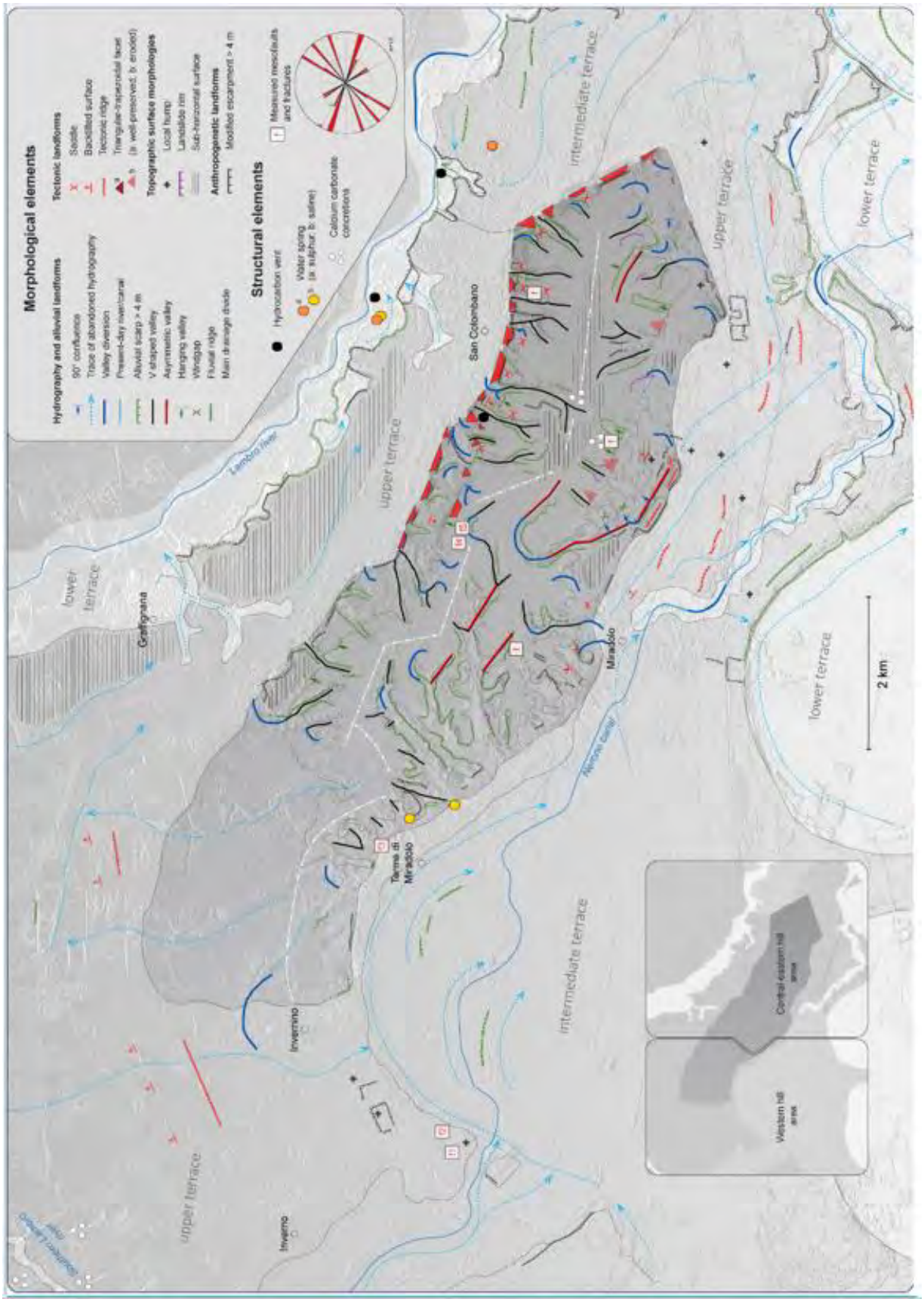

Fig. 2 – Morphological features and measured meso-structures of the San Colombano hill area, mapped on the 5 m DTM of Lombardy region (www.geoportale.regione.lombardia.it).

4.1 Western hill area: remnants of a proto-hill and adjacent terraced plains

The western San Colombano hill is characterized by curvilinear, irregular hillslopes associated to the highest values of J (J>1.5; geomorphic segments S_{15}-S_{16} in Fig.3-A). The convex-up hilltop gently dips NW and gradually links to the adjacent plain owing to colluviation and fan aggradation at the hill-toe. The sedimentary succession of the NW hill preserves the most complete pedo-stratigraphic sequence of the study area. Above the alluvial sediments of CPS1 (Fig.1-B), two superimposed loess units occur (ascribed to MIS4 and MIS2, in ascending stratigraphic order) with interposed paleosols (Zuffetti et al., 2018b). The western hill is crossed by four drainage basins of maximum IV order (*sensu* Strahler, 1957; dashed divides nr. 46-49, Fig.3-A), which are mostly abandoned at present. They are long and little incised (1.8-2.5 km in length; 0.5-1 m-high scarps). Their mouths have been located at the boundary between the hill and adjacent plain (S_{16}, Fig.3-A), since it is not possible to clearly recognize their continuation to the North, due to anthropic canalizations. All the streams strike to NW and show broad convex profiles; the relict of N060E-trending watershed at their head is cross-cut by a S-ward-concave drainage divide (Fig.2). South of it, basins are drained by low-rank centripetal streams which are entrenched between 1 and 1.5 m-high scarps, locally filling v-shaped valleys (40-45, Fig.3-A; max. length 700 m; average areal extent 0.1 km^2). Cross-cut relationships suggest that headwater erosion of these centripetal, small basins superimposed over the wider, NW-ward draining paleo-valleys.

The hydrographic systems of the western hill drain towards two different surfaces of the adjacent plain. To N and W, the hill-draining streams join the upper terrace surface of the plain (Fig.2, Fig.4-A). This surface rises 75-70 m a.s.l., gradually dips SE-wards, and corresponds to the top of the weakly-pedogenized alluvial sediments of INS (Fig.1-B). The LGM age of deposition of these sediments relies on radiocarbon date of 22015-21435 cal BC, obtained from woody particles hosted in sand-mud sequences in the study area (Zuffetti et al., 2018b), and correlate in the subsurface with sediments hosting wood fragments dated to 20785-19909 cal BC just North of the study area (Baio et al., 2004; Bersezio et al., 2004; Zuffetti, 2019). INS terraces CPS2 alluvial sediments yielding a radiocarbon age of 27648-26884 cal BC (Zuffetti et al. 2018b) INS deposits are cross-cut by sets of sub-vertical fissures striking N010E, N110E and N150E (f1-f2; Fig.2), which are filled by unweathered soft sediments, coarser than the hosting sands.

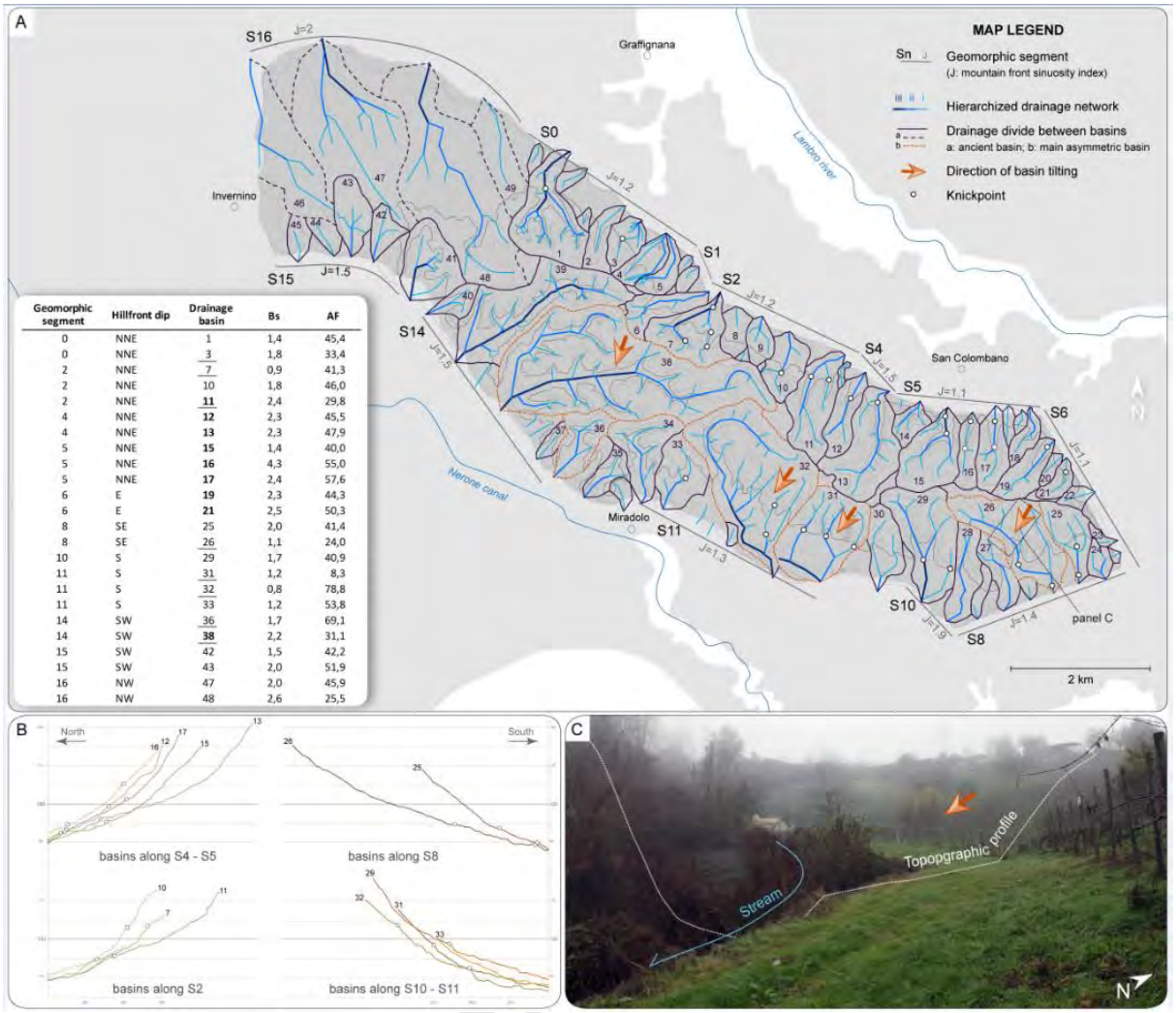

Geomorphic segment	Hillfront dip	Drainage basin	Bs	AF
0	NNE	1	1,4	45,4
0	NNE	3	1,8	33,4
2	NNE	7	0,9	41,3
2	NNE	10	1,8	46,0
2	NNE	**11**	2,4	29,8
4	NNE	**12**	2,3	45,5
4	NNE	**13**	2,3	47,9
5	NNE	**15**	1,4	40,0
5	NNE	**16**	4,3	55,0
5	NNE	**17**	2,4	57,6
6	E	**19**	2,3	44,3
6	E	**21**	2,5	50,3
8	SE	25	2,0	41,4
8	SE	26	1,1	24,0
10	S	29	1,7	40,9
11	S	31	1,2	8,3
11	S	32	0,8	78,8
11	S	33	1,2	53,8
14	SW	36	1,7	69,1
14	SW	**38**	2,2	31,1
15	SW	42	1,5	42,2
15	SW	43	2,0	51,9
16	NW	47	2,0	45,9
16	NW	48	2,6	25,5

Fig. 3 – The hydrography of the San Colombano hill. A) Drainage network and sub-basin divides. Table: selected morphometric features of the numbered basins. S_0–S_{16}: geomorphic segments (see text for discussion); Bs: basin shape; AF: asymmetry factor. Bold numbers highlight narrow-elongated basins (high Bs values); underlined numbers refer to the most asymmetric basins. B) Selected longitudinal stream profiles across the central-eastern hill (labels as in panel A). Knickpoints (white dots) are distributed at comparable elevations in adjacent streams and locate on triangular facets (compare to Figure 2). C) S-ward deepening asymmetric valley of basin 26.

Geomorphic anomalies in the upper terrace were detected at the plain-hill transition, where the topographic surface dips 10° NW, opposite to the regional SE-ward dip of the plain (Fig.4-B). Across the same boundary: i) one of the N-ward draining streams of the hill bends to SW; ii) a N-S paleo-stream cross-cutting the upper terrace and formerly draining South, is mildly deformed by an E-W ridge (Fig.2, dashed black line in Fig.4-A, 4-B) and split into two abandoned segments with opposite dip, losing its physical continuity.

The western hillslopes and the adjacent upper terrace are cross-cut by the intermediate terrace (71-66 m a.s.l.; 2-5 m high escarpments; Fig.2, Fig.4-A), formed by the alluvial deposits of the PSS (Fig.1-B). The intermediate terrace comprises two northern paleo-valleys, tributary of a wide surface cutting the southern slopes of the

western hill. This surface is bounded by a SW-concave scarp (S_{15}-S_{14}, Fig.3-A), shows a partly-preserved ridge-and-swale topography (concentric, S-ward concave ridges and swales, 100-500 m long and 1-2 m high, parallel to the terrace scarp) and progressively dips SSE-wards (Fig.2). These landforms are interpreted as the reworked relicts of the ridge-and-swale morphology of km-scale alluvial point bars (Leopold and Wolman, 1957; Leopold and Tricard, 1967), set within an abandoned meander which is comparable in size and shape to the Holocene meander loops and point bars of the Po River. The present-day anthropogenic Nerone canal has been adapted to flow within the swales, after the abandonment of the confluence between the northern paleo-valleys and the abandoned meanders on the intermediate terrace (Fig.2). Four km South of the western hill, the intermediate terrace is cross-cut by the external scarps of the lower terraces of the Holocene Po valley, max 15 m high, which host the POS (Fig.1-B; Fig.2). The lower terrace is formed by a set of surfaces bounded by up to 5 m-high, S-concave minor scarps which lower towards the present-day Po riverbed.

Summary and interpretation: geomorphic history of the western hill area. The geomorphological setting of the western hill area reveals superposed patterns of erosion (palimpsest drainage pattern *sensu* Howard, 1967), since relicts of valleys of different ages are cross-cut by different patterns. The absence of Late Pleistocene glacio-fluvial sediments (CPS2 and INS) above the CPS1 alluvial sands over the western hill (Fig.1-B), suggests that it had been uplifted after CPS1 deposition (Late Pleistocene-MIS4). In fact, from that time and onwards, only loess sediments aggraded, stabilized and weathered during the subsequent glacial-interglacial stages at this site (Zuffetti et al., 2018b). Cross-cut relationships between the Late Pleistocene loess-soil stratigraphy and the NW-draining, wide and hierarchized paleo-valleys (46-49, Fig.3-A), suggest that considerable water discharge was yielded by the existing, more elevated hill sectors to the SE, since the Latest Pleistocene. At present, this drainage network is inactive, cross-cut and superimposed by the centripetal, S-ward draining valleys. This suggests response to a local base-level drop South of the relief, owing to differential uplift. The S-ward drainage might have started to develop and to entrench since the post-glacial age of the PSS which originated the intermediate terrace (Fig.1-B). At that time, the paleo-Po River terraced the San Colombano relief shaping large meanders (curvature radius up to 1.5 km, Fig.4-A) with sandy point bars. Suggestions of post-glacial tectonics at the SCS (Fig.1-A) derive from the anomalous deformation of the upper terrace, i.e. the mentioned splitting of the N-S paleo-stream West of the hill (Fig.4-B), and from the asymmetrical meander development of the Po River system in the lower terrace (*sensu* Schumm et al., 2002). The pattern of directional scroll traces (Fig.2) results from SE-wards Po River migration during post-glacial-Holocene times. These features suggest the tectonic growth of a gentle E-W-trending ridge (Fig.4-B). It might have acted as a watershed, splitting the paleo-tributary of the Po River, leading to the capture of the hill-

draining rivers and to the progressive S-wards shifting of the Po River. In addition, the fissuring and colluvial infilling post-dating the deposition and weathering of INS (LGM), point to post-glacial faulting (Burbank and Anderson, 2013; "neptunian dikes" by Montenat et al., 1991, 2007), consistent with active differential uplift and local extension.

In synthesis, the western side of the San Colombano hill is interpreted as the relict of a Late Pleistocene, pre-MIS4 proto-hill, which was successively lowered with respect to the present-day, more elevated eastern sectors. As a consequence, its drainage pattern was offset and tilted. A S-ward draining array of small and recent basins cross-cut the former N-wards draining ones, concurrently with the S-ward- and downward-shift of the latest Pleistocene-Holocene bends of the Po River. This occurred in steps, corresponding to the intermediate terrace of the latest Pleistocene PSS and to the lower terraces of the Holocene POS (Fig.1-B).

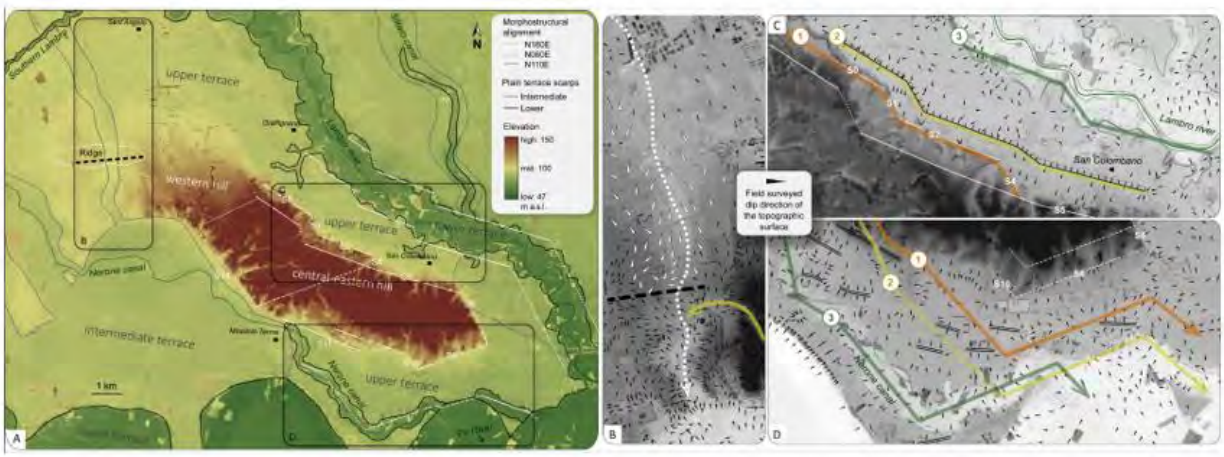

Fig. 4 – The hydrography of the plain adjacent to the San Colombano hill. A) DSM of the study area highlighting the main directions of (paleo-) river traces compared to the hillslopes orientations. S_0–S_{16}: geomorphic segments as in Fig. 3. Black frames: location of panels B-C-D. B) The western study area: anomalous N-ward dip of the plain adjacent to the hill (compare white-black triangles). C) Terraced plain N of the central-eastern hill. 1 to 3: interpreted chronology of the mapped scarps. D) South of the hill: N110E-trending ridges (black double lines) separate elongated incisions. 1 to 3: interpreted chronology of paleo-river shifting towards SW.

4.2 Central-eastern hill area: a composition of fault-blocks

The central-eastern San Colombano hill (max. elevation 146 m a.s.l.) is framed by straight, steep and rectilinear slopes, often associated to polygonal facets, which get progressively more irregular and gentle westwards (Fig.2, Fig.3). On the adjacent plain, the entrenched valleys of the lower terrace mimic the orientations of the straight hillslope segments, with abrupt diversions (Fig.4). Since the contrasting features among the central-eastern hill area relate to the orientation of the three mentioned sets of morphostructural lineaments (Fig.1, Fig.2), the description hereafter will follow these elements.

4.2.1 Relicts of F1-F2-bounded blocks

The central-eastern hill preserves morphostructural evidence claiming for N160E- and N060E-trending fault sets. Two N060E elevation divides bound the central, western and eastern hill morphologies (Fig.2). Thermal and mineralized water springs occur at the intersection between the western N060E divide and N160E hillslope at Terme di Miradolo (Fig.2), where a set of 160/70 and 340/80 dipping, conjugate normal faults dissect the CPS1 (f3, Fig.2). These meso-faults display 20 cm vertical throws and can be related to a N060E-trending structural set. In the central-eastern hill, river bending, aligned left-lateral stream captures, *sensu* Huang (1993) and Gaudemer et al. (1989), and segmentation of the main hill watershed occur at the N060E divide. The widest, highly-asymmetric basins of the central hill are elongated along the same orientation. They drain SW-wards, orthogonal to the N160E-striking hillslope (S_{14}, Fig.3-A), and host more than 30 m-deep, wide valleys. They are commonly associated to the highest-rank incisions composing an irregular to dendritic pattern (max IV order; basins 38-39, Fig.3-A). Evidence of a rectangular pattern only occur in correspondence of N110E, S-dipping asymmetric valleys, which parallel the central hill drainage divide (Fig.2, Fig.3-A). The stream network locally cuts the relicts of NW-SE paleovalleys, incised within the alluvial CPS1. One of them hosts CPS2 deposits (Fig.1-B), formed by an alluvial unit covered by a colluvial fill which marks the abandonment of the valley. Paleocurrent trends of the alluvial unit indicate NW-SE-wards flows; paleosol clasts indicate reworking of MIS5 paleosols from a northwestern source (Zuffetti et al., 2018a, b, c).

The rectilinear easternmost slopes of the hill strike N060 and N160, with a low mountain front sinuosity index ($1.1<J<1.4$; S_6-S_8, Fig.3-A, Fig.5). The N160E-trending slope (S_6) is characterized by the lowest J and by a single array of well-defined, 40 m-high polygonal facets, steeply dipping to NE. Right-lateral valley deflections occur along the facets (Fig.2). Conversely, relicts of strongly-degraded, 20 m-high facets occur at about 105 m a.s.l., along the N060 hillslope. Here, knickpoints locate along SE-ward draining, parallel streams (basins 24-29, Fig.3-A-B).

The eastern hilltop is a planar, sub-horizontal surface (Fig.2, Fig.5) which truncates the fluvial sediments of CPS1 and is blanketed by a loess attributed to LGM by Zuffetti et al. (2018b; L, Fig.1-B). It corresponds to the relict of an uplifted planation surface, originated in an alluvial setting during the spreading of the MIS4 glacio-fluvial systems (Zuffetti et al., 2018b, c), i.e. coeval to the development of the mentioned paleo-valleys of CPS2 in the central hill. At present, this flat-top surface is offset and downthrown by about 70 m to the North of the hill, where a deep truncation surface cut into CPS1 has been surveyed in shallow excavations a few meters below the top of the upper terrace (Fig.1-B).

Coupled N060E-N160E morphostructural alignments characterize the plain South of the central-eastern hill, where analysis of dip of the topographic surface highlights abrupt bending of some NW-SE-directed paleo-incisions (Fig.4-D). The widest and most entrenched southernmost one, run by the present-day Nerone canal, is cross-cut by the recently-abandoned meanders of the Holocene Po River (lower terrace, Fig.2, Fig.4-D). Comparable features are lacking in the plain North of the central-eastern hill, where centripetal dip directions of the topographic surface relate to the erosional withdrawal of small tributaries of the Lambro river (Fig.2, Fig.4-C).

Summary and interpretation: geomorphic history of the F1-F2-bounded blocks. The N160E and N060E morphostructural alignments of the central-eastern hill are consistent with the F1 and F2 fault systems (Zuffetti et al., 2018a; Fig.1-B) which controlled the reorganization of the drainage network. A three-stages relative chronology can be interpreted: i) Late Pleistocene (MIS4-MIS3) incision of paleovalleys, filled by CPS2 sediments (Fig.1-B; Zuffetti et al., 2018b). NW-SE paleocurrents of the alluvial CPS2 indicate a paleo-drainage from a formerly-elevated sector, at present lowered in the western hill. Terracing of the CPS1 gave origin to the planation surface whose relicts form the top of the present-day eastern hill. This surface is a morpho-stratigraphic marker of the fault displacement at the eastern hill fault-block, relatively to the formerly-uplifted plain. ii) Establishment of a N160E and N060E-trending drainage network. The latter cross-cuts the CPS2 paleovalleys and was probably controlled by F2 faults. Shape, width and depth of these N060E valleys are coherent with a high-energy stream network, probably related to a high elevation of the source area (not preserved at present). iii) Dissection along the N110E morphostructural lineaments. The central hill watershed and N060E draining basins were abruptly cross-cut by N110E-oriented lineaments, along which a set of parallel streams developed. This relationship suggests the late reorganization of the hill morphology, controlled by N110E-trending structures (F3, Fig.1), as it will be detailed in the following section.

4.2.2 F3-bounded blocks

The central-eastern hill is characterized by the straight and faceted shape of the N110E-trending northern and southern slopes (Fig.1-B, Fig.2). The N110E morphostructures always cross-cut the N160E- and N060E-trending landforms. Symmetric, parallel and small basins orthogonal to the N110E faceted hillslopes cross-cut the N060E-oriented basins of the central hill (1-10, 33-37, Fig.3-A). Equally, the northern basins draining the eastern hill (1-18, Fig.3-A) are straight and parallel, displaying an average areal extent of 0.2 km^2. They comprise short (average length 180 m), poorly-hierarchized streams (max II order) with V-shaped valleys incised down to the slope scarps. One array of knickpoints is observed in proximity of the N and E toes of the eastern hill; two parallel arrays of

knickpoints locate along the N-draining streams of the central hill and along the S-draining ones of the eastern hill (Fig.3-A). Right-lateral valley deflections occur along the N110E straight borders of the hill (S_0, S_2, S_5, S_{11}, Fig.3), and are frequently associated to the remnants of perched valleys (Fig.2, Fig.5-A). These paleo-drainage relicts are preserved above the most elevated, N110E-trending hillslopes of the central hill.

All the N- and E-ward draining streams cut across rectilinear hillslope segments, with low mountain front sinuosity index ($1.1<J<1.4$; Fig.3-A, Fig.5). The lowest values characterize the northern fronts (striking N110E; S_0-S_5) and the eastern ones (N160E; S_6), which show alignments of continuous and well-defined triangular and trapezoidal facets (60:40 relative proportion; Fig.2, Fig.5-A). The northern slope shows two parallel arrays of N-dipping facets, 15 to 20 m-high each in the central hill; a single array of facets, oriented N110-to-N080E and reaching 50 m in height, faces the San Colombano town (S_5). Above it, a N110E-trending array of saddles occurs (Fig.5-A).

Dip-slip extensional conjugate mesofaults were measured in the central hill (f4, f5, Fig.2), consistent with N110E-striking systems. Some N110E-elongated hill terraces are bounded by two sets of polygonal facets and elevate at about 90-100 m a.s.l. (Fig.2). Locally, these surfaces are gently back-tilted towards the upper array of facets (Fig.5). Along the northern hillslopes, these terraces are formed by the LGM glacio-fluvial sediments of INS with a loess blanket on top (Fig.1-B). Local colluvial wedges occur below the loess at the steepest hillslopes, suggesting tectonic-driven colluviation along F3 faults (Zuffetti et al., 2018b). The different elevation of the INS terraces and their low thickness (cross-section, Fig.1-B) indicate latest Pleistocene syn-depositional activity of the F3 structural set, which down-threw the hanging-walls to the North. In the eastern hill, landslides are frequent; their rims are usually NW-SE-oriented, inducing S- and SW-ward mass movements. Deep (>2 m) multiple gullies develop at the highest elevations, producing a disconnected network of channels that dissect the hillslope and increase soil erosion.

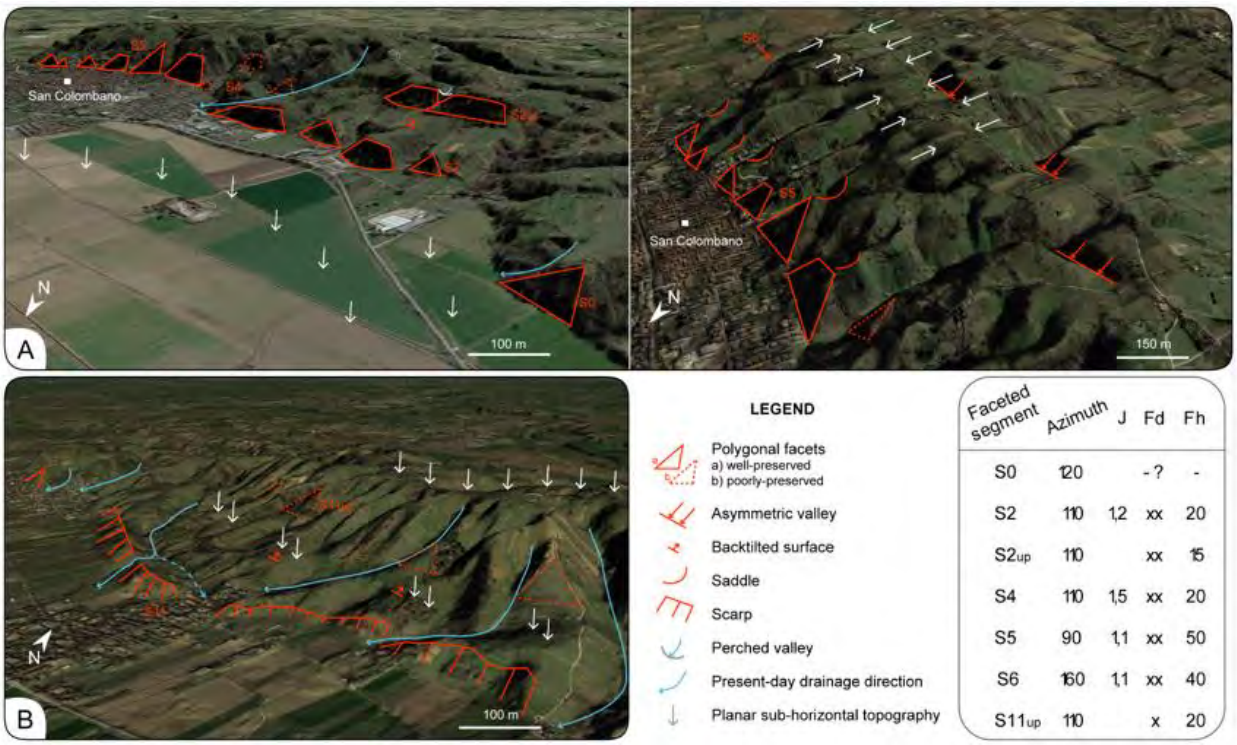

Faceted segment	Azimuth	J	Fd	Fh
S0	120		-?	-
S2	110	1,2	xx	20
S2up	110		xx	15
S4	110	1,5	xx	20
S5	90	1,1	xx	50
S6	160	1,1	xx	40
S11up	110		x	20

Fig. 5 – The San Colombano hillslopes and hilltop. A) Detail of triangular and trapezoidal facets bounding the northern flank of the hill, observed from the North-West and West (left- and right-hand side panel, respectively). B) Hillslope morphology along the southern side of the hill, observed from the South-East. Valley diversions (curved arrows) are common at the straight hill boundaries. Google Earth views, vertical exaggeration 3x. S_0-S_{11up}: reference faceted hill front segments presented in the box at the right-hand side. J: mountain front sinuosity index; Fd: degree of facet development (x: low, xx: high); Fh: facet height in meters.

The S-ward draining basins are wider (average area 1 km^2) than the symmetric N-ward draining ones, and can reach the III order. Their slopes lower in dip between 110-105 m a.s.l, where lined-up knickpoints occur along the streams (Fig.3), together with strongly degraded relicts of N110E-striking triangular facets (15-20 m high;S_{11up}, Fig.5-B). The latter bound sub-planar surfaces around 90 m a.s.l., exposing the Late Pleistocene CPS1. These are frequently back-tilted towards the facets and crossed by N120E-oriented windgaps (Fig.2; Fig.5-B). S-ward draining streams either parallelize their headwaters along the N110E main drainage divide; Fig.3-A), or develop N110E asymmetric valleys deepening S-ward (Fig.3-C). Relicts of hanging valleys and orthogonal confluences occur on the S-ward dipping flanks of these valleys.

Two groups of convex-up torrential fans result from the intermittent discharge by the dense channel network crossing the hill since the latest Pleistocene (MLS; Fig.1-B; Fig.3-A). On the southern hillside, fans are $6*10^4$-$1*10^5$ m^2-wide, dipping less than 10°; most of them are coalescent. Differently, at the toe of the faceted N110E northern slope, fans have smaller areas ($2*10^4$-$4*10^4$ m^2), steeper surface (18°) and form thicker sediment prisms than the southern ones.

Several features of the alluvial terraces around the hill are closely linked with the morphostructures of the relief. The upper terrace to the North of the eastern hill includes two orders of surfaces, bounded by 1-2 m-high scarps parallel to the faceted hillslope (S_0-S_5, N110E-N160E trends, Fig.4-C). The lower terrace segments of the Holocene Lambro river valley mimic, in length and direction, the same array of rectilinear segments (Fig.4-A). Thermal and mineralized water springs occur along the these river tracts, and along the N160E southern hillslopes (Fig.2). Hydrocarbon and saline water vents are common both on the Lambro river scarps and in the deep valleys crossing the central hill (Fiorani Gallotta, 1921). South of the central-eastern hill, the upper terrace (INS, Fig.1-B) shows several *en-enchelon* N110E-oriented rectilinear ridges with interposed back-tilted surfaces (Fig.2, Fig.5-D).

Summary and interpretation: geomorphic history of the F3-bounded blocks. The tectonic control by N110E and N160E lineaments is envisaged in the morphostructural framework of the central-eastern hill. These lineaments are highlighted by steep topography (N-ward dipping set of northern facets, Fig.5) accompanied by slope breaks along transverse profiles (location of knickpoints, Fig.3). They contribute to delineate the F3 and F1 faults systems which offset the Pleistocene stratigraphy and structures (Fig.1-B). Also the incoherent asymmetry of the drainage and of the topographic features claims for tectonic explanations. Aligned river captures indicate river response to the tectonic offset between fault-blocks, and the consequent adjustment of the stream network to the changes of the slope gradient. Cross-cut relationships suggest that the stream pattern draining the northern hillslope originated under fault control; uplift of the southward footwall of F3 faults enhanced N-ward draining stream incision which, in some cases, cross-cut the older N060E drainage basins (38-39, Fig.3-A). The perched valleys punctuating the N110E-trending arrays of facets, strengthen this interpretation. The rectilinearity and dip of the N110E- and N160E-striking faceted spurs are consistent with the tectonic activity of the F3 and F1 structural lineaments. The simple, parallel drainage pattern of the eastern hill is easily associated to tectonic activity along F3 faults: rapidly-uplifted mountain fronts generally produce elongated, parallel, steep basins (Bull, 2007), which are the drainage features of the northern hillslopes. Widening of the basins occurs from the mountain front and upwards during waning tectonic activity (Ramírez-Herrera, 1998). The asymmetry among the wide basins of the southern hill and the small, elongated basins of the northern side (Fig.3-A), may relate to higher rates of tectonic displacement along the northern array of F3 faults. This interpretation is also supported by the higher degree of preservation of the northern polygonal facets than the southern ones (Fig.5), the deepening of N-ward draining valleys orthogonal to the northern hill front (Fig.3), and the constant orientation of asymmetric valleys dipping S-ward (Fig.2). The very low values of J (Fig.3-A) fit with this interpretation: during rapid uplift, the mountain–piedmont junction remains straight and the valley floors narrow even where rocks are soft (Bull, 2007), as it occurs

at the San Colombano hill piedmont.

Several studies demonstrated that river long profiles are very sensitive to tectonic perturbations, which can produce knick-point discontinuities in the profile (Spagnolo and Pazzaglia, 2005; Whittaker et al., 2008). Knickpoints location along the streams crossing the N110E-oriented hillslopes coincide with the location of F3 faults (Fig.2-Fig.3). The distance between the knickpoints and the main watershed, lower along the northern streams than on the southern ones, suggests the northern F3 fault system as the most recently active. The cross-cut relations between morphostructures related to F3 and the older, F1-F2 fault systems, support this interpretation. On the southern hillslope, the alignment of windgaps (Fig.2) identifies the steps of fault-driven down-throw of the N110E-striking eastern hill blocks. Also the N110E-oriented ridges, and back-tilted surfaces on the upper terrace to the South, are coherent with faulting along F3.

5. Late Quaternary palimpsest landscape evolution

The Late Quaternary tectonic activity along conjugate fault-sets in the study area (Fig.6) is documented by the geomorphic features, the tectonic structures and associated deep fluid vents (Fig.1-B; Fig.2), the offset of the Quaternary stratigraphy, and the redeposition of paleosols.

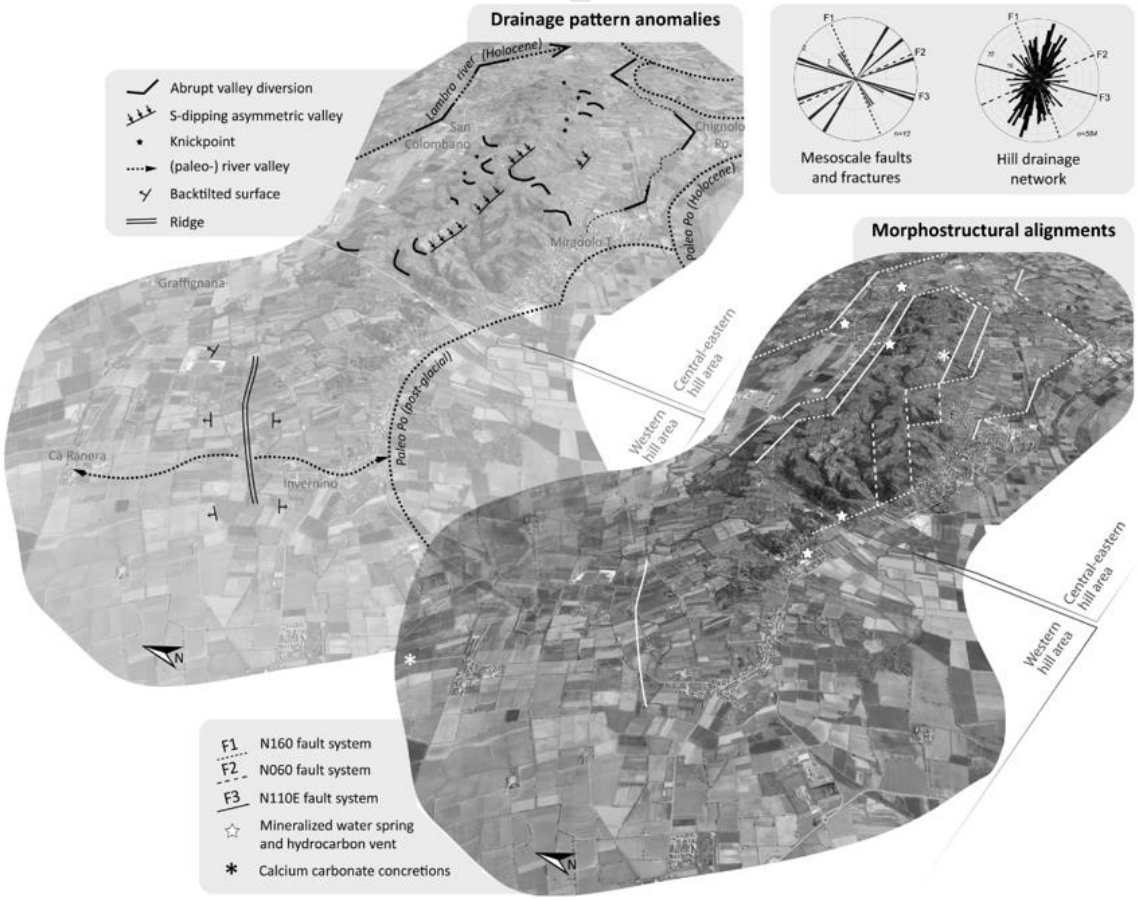

Fig. 6 – Perspective views of the topography of the San Colombano hill, highlighting the relationships between the main morphostructural elements and the interpreted fault systems F1, F2, F3.

Ongoing relative uplift of the SCS fault-blocks is highlighted by the N160E- and N110E-oriented regressive headwater erosion that affects the N-S trending hill streams and by the active gravitational processes, in keeping with the geodetic data (Arca and Beretta, 1985; Scardia et al., 2012). A Late Quaternary relative uplift rate of about 0.5 m/kyr can be approximately inferred for the SCS on the basis of: i) the cumulative displacement of the relict planation surface at the hilltop vs. the correlative unconformity down-thrown by 70 m in the adjacent plain; ii) the hill-front morphologies, in agreement with literature data concerning the comparable active fault-bounded ranges (Bull, 2007; McCalpin, 2009).

The geomorphic features of the plain (Section 4) document a never-observed palimpsest of hydrographic anomalies and cross-cut relationships between different terraced surfaces. Their orientation reflects the tectonic/morphostructural systems of the hill suggesting a paired evolution (Fig.7). According to these new observations, the "Plain Main Level" of the Po Plain (Castiglioni and Pellegrini, 2001) can be reinterpreted as a composite, polygenic geomorphic unit, in keeping with Bini et al. (2015), affected by the same tectonic increments recorded on the adjacent hill.

The orientation and kinematics of the here-interpreted local faults is coherent with Riedel fault assemblages, related to the elements of the Emilia Arc. These are the sinistral Pavia-Casteggio lateral ramp (PCLR) and a dextral transfer fault between the San Colombano and Casalpusterlengo-Zorlesco adjacent structures (CZTF, Fig.1-A; Fig.8).

Post-LGM tectonics in the Central Po Plain has been investigated in the regional entrenchment and diversions of the main rivers (Burrato et al., 2003) and the local deformation at the Romanengo hill (Bresciani and Perotti, 2014), and related to a late compressional regime linked to the N-ward advance of the buried arcs of the Apennines. Location and focal solutions of historical earthquakes (Vannoli et al., 2015 with references; Fig.1-A), and evidence of Holocene inverse faulting at the meso-scale (Zanchi et al., 2019), indicate recent compressional activity about 8 km North of the study area (Alps-Apennines interference zone; CPPS, Fig.1-A; Table 1). At the Alpine margin of the basin, the isolated reliefs South of Brescia (CCS, Fig.1-A) show Late Quaternary uplift, folding and faulting as surface expressions of Southalpine blind thrusting (Livio et al., 2014; Table 1). All of these findings testify that the Late Quaternary interference between the N-wards propagation of the buried Apennine fronts and the Southalpine structures played a basin-scale role in the morphotectonic evolution of the intervening foreland,

and must be considered to interpret the site-specificity of the Apennine-related intra-basin reliefs. Peculiar features of this setting are the buttress effect of the Alps-Apennines interference zone (CPPS, Fig.1-A), the activation of transfer zones between thrusts, and the location and timing of extension. According to several Authors, the migration of extensional-and-compressional structural domains characterizes the evolution of different sectors of the Apennines orogen (Liotta et al., 1998; Picotti and Pazzaglia, 2008; Bennett et al., 2012; Molli et al., 2018); its contribution to progressive landscape changes at the Po Plain-Apennines morphological front since the Late Pleistocene cannot be neglected. In this work, stratigraphic relationships and OSL-^{14}C age determinations, permitted to integrate the geomorphological and geological evidence into a chronology of Late Quaternary morpho-tectonic and depositional increments along the Emilia Arc and the SCS.

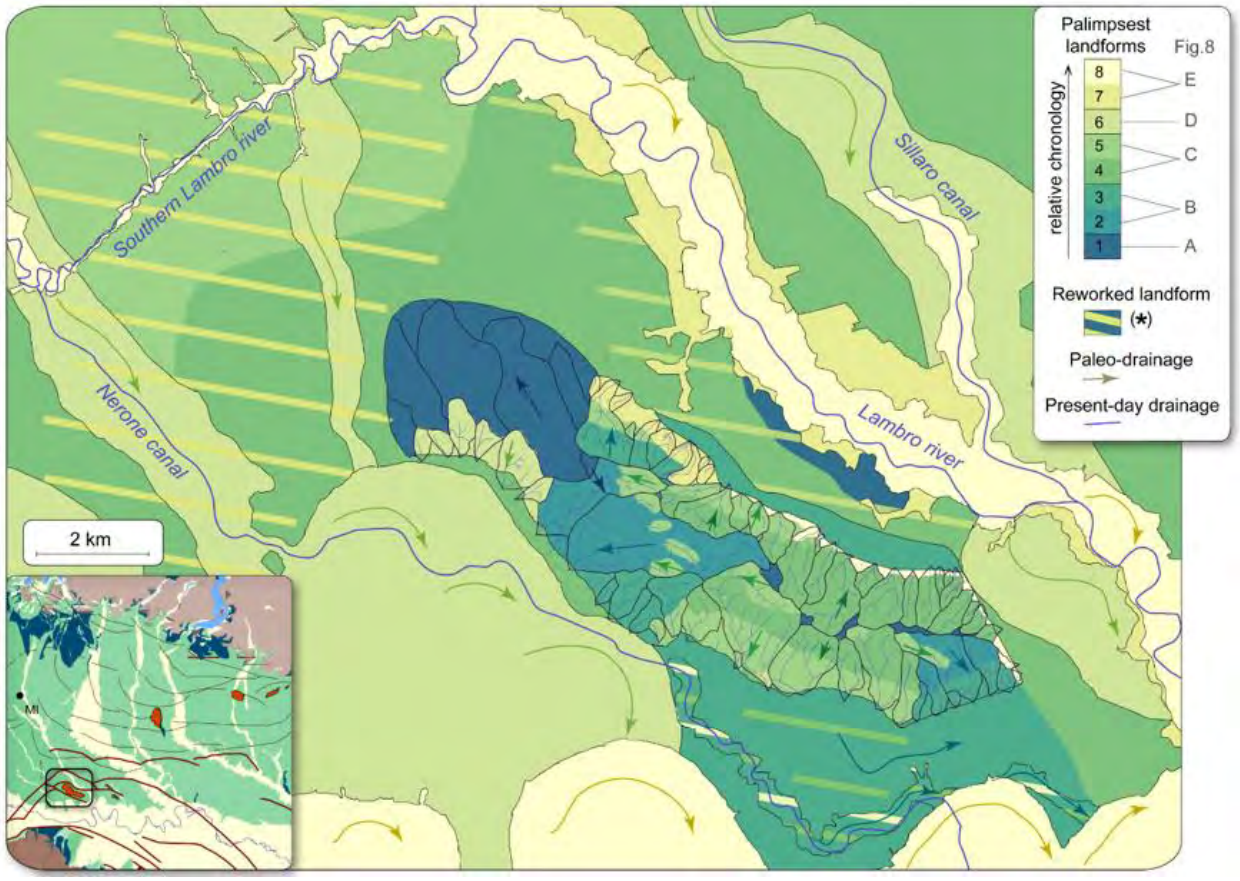

Fig. 7 - The palimpsest landscape of the San Colombano hill area. Colour scale: interpreted relative chronology of the landforms of the hill and adjacent terraced plain. Arrows: direction of the paleo-drainage. Line marks (*): the colour of the oblique bars refers to chronology of reworking of the plain terraces (in solid-fill colour) following the general colour scale of the map. Letters A-E relate each landform to the stage of morpho-tectonic evolution presented in Fig. 8. Description of the landscape units in Section 4. Left-hand corner: location of the study area in the structural framework of the Po foreland basin (legend as in Fig.1).

5.1. Morpho-tectonic evolution

A sequence of five Quaternary evolutionary increments (Fig.8) is proposed for the origin of the present-day palimpsest landscape of the SCS (Fig.7).

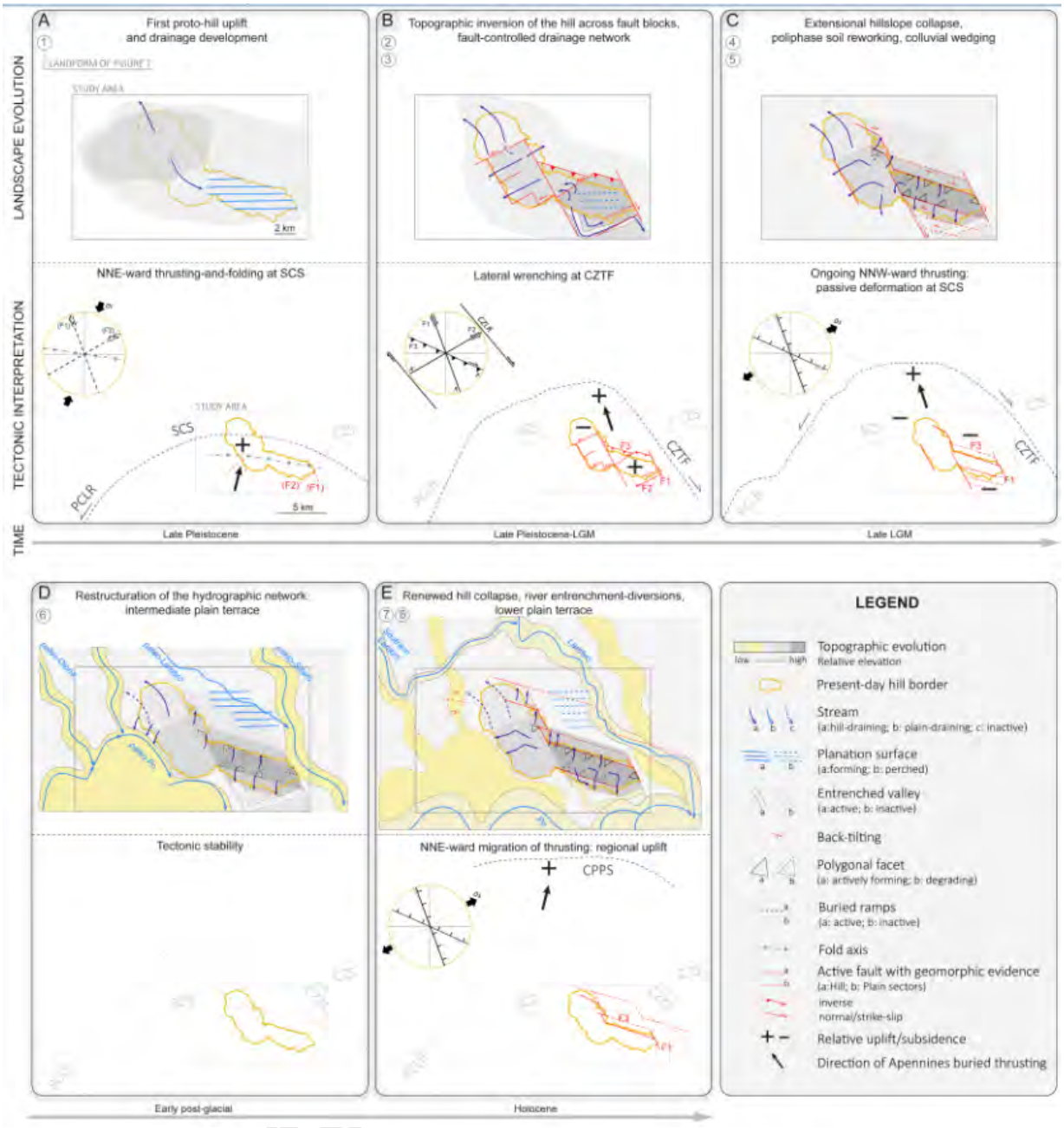

Fig. 8 – Late Quaternary evolution of the San Colombano hill landscape, and its relationship with the interpreted evolution of the Northern Apennines deformation front. The study area is framed by the black rectangle. Upper corner on the left-hand side of each panel: kinematic interpretation of the major active structural trends. Labels of the Apennines structures as in Fig. 1. Encircled numbers: landforms mapped in Fig. 7 whose origin derives from the here-presented increments.

5.1.1 First proto-hill uplift: NNE-ward thrusting-and-folding of the SCS. During the Late Pleistocene, NNE-ward propagation of the buried Emilia Arc induced re-folding of the former Mio-Pliocene ramp fold, which had been already cut and sealed by the Gelasian Unconformity (Fig.1-B). During this step, a first proto-hill was uplifted above the average elevation of the alluvial plain (Fig.8-A). Its remnants are preserved in the present-day western hill sector (Section 4.1; Fig.7: landform 1). The Late Pleistocene CPS1 terraced the structural culmination giving origin to the tectonic-induced Middle-Late Pleistocene Unconformity (Fig. 1-B; Zuffetti et al., 2018a). The on-going uplift

of the proto-relief was accompanied by valley incision within the Mio-Pleistocene substratum (MIS4-CPS2 syn-tectonic paleovalleys of the western sector; Fig.1-B). To the East of the western proto-hill, the CPS2 river network eroded a planation surface (Fig.8-A).

This thrusting increment was plausibly driven by the PCLR (Fig.1-A; Fig.8-A), resulting in a N110E-striking anticline. The fold is coherent with NNE-ward propagation of thrusting and with left strike-slip along the PCLR, consistently with the paleo-stress orientations proposed by Benedetti et al. (2003). Extensional faults parallel to the fold hinge, and conjugate shear planes on the fold limbs, are the expected accompanying structures (Ramsay and Huber, 1987). The orientation of F1 (N160E) and F2 (N060E) fault sets suggests that they might have formed as a conjugate system during this increment, predisposing the tectonic anisotropies that will condition the future increments (Fig.8-A).

5.1.2 Topographic inversion of the hill: origin of the fault-blocks. During deposition and weathering of CPS2 (MIS4-MIS3), differential uplift initiated (Fig.8-B). Conjugate F1-F2 fault sets separated different morphostructural blocks, which started to evolve independently: i) the western hill was lowered with respect to the central-eastern hill, where wide valleys started to develop along gentle slopes (Section 4.1); ii) the CPS2 paleo-valleys of the western proto-hill sector were deactivated and cross-cut by N060E-trending valleys, controlled by the active F1-F2 fault system (Section 4.2; Fig.7: landform 2); iii) the planation surface of the eastern hill started to be uplifted above the surrounding alluvial plain (Fig.8-B). The weathered relicts of this surface are preserved on the top of the present-day eastern hill (Fig.5-A and Fig.7). The uplifting block was wider than at present: S-ward draining streams continued in the plain, where they were diverted along F1-F2 sets and shifted toward the paleo-valley currently drained by the anthropic Nerone canal (Fig.4-D). Differential uplift lasted up to MIS2, during which the terraces of rivers, sourcing from the LGM alpine glaciers (INS), were deposited, segmented, and uplifted on the flanks of the relief (Fig.1-A).

This evolution is interpreted as a result of dextral wrenching along a transverse fault zone, which dragged the central-eastern hill sector towards NNW (Fig.8-B). It could relate to slip along a dextral transfer fault zone adjacent to the SCS (CZTF, Fig.8-B), which reactivated the inherited F1-F2 structures, induced uplift along N110E-trending F3 reverse faults and displaced the INS terraces. The interpreted conjugate fault system inducing lateral wrenching and dissection of the SCS, is consistent with NNW-ward propagation of the SCS. The Late Pleistocene chronology and kinematics of the CZTF fits with the interpretation of Benedetti et al. (2003), who also suggested Late Pleistocene reactivation of a thrust 20 km South of the present-day hill (BSF; Fig.1-A), and finds a good chronological correspondence with the thrusting stages proposed for the pedeapennine border by Frigerio et al.

(2017) and Maestrelli et al. (2018).

5.1.3 Late LGM collapse of the hill along F1-F3 faults. The central-eastern hill started to collapse during latest Pleistocene (MIS2), along F1-F3 conjugate fault systems. They cross-cut the former (morpho-) structures and induced the reorganization of the drainage patterns (Section 4.2; Fig.7: landforms 4-5; Fig.8-C). The oldest INS terraces were back-tilted S-wards and downthrown towards the plain, along the faceted slopes, following the right-stepping of the F3 fault surfaces. The new, parallel, NNE-SSW drainage pattern superimposed on the former N060E-trending one (Fig.7). Syn-tectonic colluvial wedges reworking MIS5-MIS3 paleosols covered the fault hanging walls (Zuffetti et al., 2018b). Ongoing wrenching at the dextral CZTF plausibly drove the N-ward migration of the SCS deformation front. The active F3 and F1 fault sets, refreshed the polygonal facets and enhanced stream entrenchment. On the southern hill side the former morphostructures were progressively inactivated and drainage was diverted and cross-cut by N110E-trending asymmetric valleys (Fig.7). Conjugate sets of normal faults affecting CPS1 and INS (f1-f2-f4, Fig.2) document local extension after σ1-σ2 permutation.

Considering the current regional schemes for the Quaternary evolution of the Apennine Emilia Arc (Boccaletti et al., 2011 and references), a Latest Pleistocene right-lateral transtension-to-extension, linked with NNW-wards movement driven by the CZTF, can be conservatively suggested. The shift of the active blind compressional front away from the relief, might have caused the permutation of the local stress field (Fig.8-C), and the reworking of the pre-existing cross-structures (F1-F3) which were in ideal orientations to be reactivated. This interpretation expands the proposal of Ghielmi et al (2013), which accounted for a change from horizontal to vertical σ1 for the Emilia Arc since the Middle Pleistocene. The here-proposed multi-deformation along inherited cross-structures is a common feature of the tectonic evolution of the axial zone of the Apennines (e.g. Pizzi and Galadini, 2009).

5.1.4 Birth of the post-Glacial intermediate alluvial terrace. During the early post-LGM the INS terrace, which contributed to form the Plain Main Level adjacent the hill, was cut by the alpine meandering tributaries of the Po River (Fig.7: landform 6; Fig.8-D). They merged with the large meanders of the paleo-Po, carved on the SW flanks of the hill, together originating the intermediate plain terrace and depositing PSS (Fig.1-B). No syndepositional paleo-drainage anomalies are observed along the northern abandoned river traces, which run following the NNW-SSE average regional gradient of topography. The same observation holds for the entire southern Po Plain of Lombardy, where several meandering traces of abandoned rivers of the same age follow the main topographic gradient (Bersezio, 1986; Castiglioni and Pellegrini, 2001; Marchetti, 2002). It suggests that the intermediate terrace formed during a phase of tectonic quiescence while the Alpine glaciers started to retreat.

5.1.5 Regional uplift and renewed hill collapse: N-ward shift of thrusting. A late step of regional uplift and collapse of the SCS is recorded during the Holocene entrenchment of the regional river network (Fig.1-B; Fig.8-E). The Holocene river valleys (lower terrace) cross-cut the abandoned traces of the intermediate-terrace rivers and show several anomalies around the SCS (Fig.7: landforms 7-8,). This holds also at the regional scale, since all the Holocene valleys of the Central Po plain suffer a well-known ESE-ward diversion in correspondence of the buried Southern Alps-Apennines interference zone (CPPS, Fig.1-A). The deformation of the upper and intermediate plain terraces NW of the SCS (Fig.4-B; Fig.6) and the progressive S-wards shifting-and-entrenchment of the Po River to the S of it, document ongoing uplift at the SCS . The entrenchment of the Lambro river valley, and its abrupt diversions along the strikes of F1-F3 fault systems (Fig.4-A), are consistent with this interpretation and suggest the prolongation of faulting below the plain landscape. At this stage, extensional collapse was pronounced mostly at the north-eastern hill-front, where the polygonal facets along F3 system were rejuvenated.

We propose that the regional river entrenchment and the related anomalies might be due to a Holocene N-ward step of the Emilia arc along a deep sole-thrust. It induced N-wards translation and passive uplift of the SCS, promoting on-going collapse of the hill. The active compression front moved N-wards, reaching the interference zone with the Southalpine thrusts (CPPS, Fig.8-E). Buttressing along this belt was plausibly responsible for the reactivation of the Southalpine thrusts at Romanengo (RS, Fig.1-A; Bresciani and Perotti, 2014). The focal solutions, the relatively-high depths of historical earthquakes in the Lodi area (Fig.1-A), and the rates of uplift in the Central Po Plain (Arca and Beretta, 1985; Boccaletti et al., 2011; Farolfi et al., 2019) support this interpretation.

6. Discussion

The palimpsest landscape of the San Colombano hill Structure reflects the polyphase foreland propagation of the external N-Apennines fold-and-thrust belt during the Late Quaternary. The new field-based observations and measurements permitted to map and describe the spatial-chronological relationships between the landforms of the palimpsest (Fig.7, Fig.8) in the peculiar foreland type of the Po Basin. The novel reconstruction (Section 5) documents the sequence of uplift, wrenching, and collapse increments induced by thrust propagation in this specific setting. In the Quaternary Po Basin, in fact, subsidence and sedimentation have been controlled by the outwards propagation of the Nothern Apennines salients since the Pliocene (Pieri and Groppi, 1981; Bigi et al., 1990; Doglioni, 1993; Ghielmi et al., 2013), but the infilling depositional systems have mostly been fed by the opposite, Alpine side (Ori, 1993; Castiglioni and Pellegrini, 2001). It differs from the majority of the foothill regions of the world, where the syntectonic depositional systems are mostly fed by the growing belt (Mouthereau et al.,

1999; Mayer et al., 2003; Yin, 2006; Malik et al., 2014; Goswami et al., 2018 among others). Moreover, the fronts of the two thrust belts interfere in the centre of the plain, a few km North of the Emilia salient and of the study area (CPPS, Fig.1-A; Bigi et al., 1990; Fantoni et al., 2004; Toscani et al., 2014), where the Apennine front is buttressed by the opponent Southern Alps. This latter chain was eventually still active, involving out-of-sequence thrust propagation far North from the belt tip, as the northern cluster of Late Quaternary intra-basin reliefs testifies (Bresciani and Perotti, 2014; Livio et al, 2014). The regional subsidence/uplift and seismological patterns (Table 1; Fig.1-A) responded to active thrusting, buttressing, flexural response of the foreland crust, and to isostatic readjustments consequent to the Quaternary glacial cycles (Carminati et al., 2003). Comparable settings are unusual among the Quaternary active foreland thrust belts worldwide, where the buttressing effects of the foreland ramp is mostly described in the case of inherited extensional structures (e.g. Morley, 1986; McClay, 1992; Ziegler and Fraefel, 2009 among others).

Hence, while the individual morphotectonic features of the studied setting are comparable to many existing instances, both from the eastern Po Basin-Adriatic foredeep, and other foreland belts (Delcaillau et al., 1998; Keller et al., 1999; Delcaillau et al., 2001; Pearce et al., 2004; Delcaillau et al., 2006; Singh, 2008; Pedrera et al. 2009; Singh and Jain, 2009; Ponza et al., 2010; Grützner et al., 2017, 2019), the resulting morphostructural palimpsest is novel. It enriches the set of reference case-histories with the polyphase chronology of a landscape, which responds to the morpho-tectono-sedimentary evolution of an advancing thrust front which is blind, basinward-buttressed, segmented by transverse faults, and fed by remote sediment sources subjected to cyclical glacial advances towards the basin depocenter. The morpho-structural elements and the stratigraphic evidence of incremental folding-and-faulting, like the colluvial wedges shed from scarps (Zuffetti et al., 2018a; 2018b), have been typically used as indicators of paleoearthquakes (McCalpin, 2009). Moreover, the described geometries and fault intersections, i.e. the places where most of the propagating rupture terminates after each seismic event (Knuepfer, 1989; McCalpin, 2009), have been considered as key-features for the assessment of seismic hazard, and applied to study the extensional faults along the Apennine chain (e.g. Pizzi and Galadini, 2009). The chronology of morphostructural events proposed in Section 5 suggests which structures are candidate to be investigated as potential sources of the recent earthquakes, both at the study site and at the regional scale. Starting from these general first hypotheses, furthermore detailed investigations on the paleoseismic potential of the studied area are encouraged by the conclusions of this work.

7. Conclusions

The work suggests the following issues on the evolution of landscapes in foreland basin settings, from both regional and general points of view:

- the palimpsest landscape of the San Colombano hill Structure describes the effects of interfering basinward thrusting and peri-glacial dynamics on landscape evolution, and mirrors the Late Quaternary uplift/subsidence patterns of the Po foreland basin. Active tectonics is driven by the southern mountain range (Apennines), while climate-controlled sedimentary sources relate to the opposite, glaciated chain (Alps).
- The morphostructures of the study area point to a Late Quaternary sequence of growth, inversion and extensional collapse of an intra-basin high. This evolution reflects the anisotropy of the active thrust belt, whose advances occurred in differently NNE- to NNW-oriented basinward steps, promoting the activation of transfer zones. The latter caused localized wrenching, consequent fault-driven topographic inversion of fault-blocks, and paired anomalies on the adjacent plain.
- Extensional collapse accompanied uplift and wrenching, contributing to redistribute and refresh the landforms along extensional fault systems. Relict depositional and morphological surfaces, and abandonment/diversion patterns of the hydrography, are the widespread outcomes of this evolution. The precise correlation between tectonic, depositional, geopedological and morphological features is necessary to define the correct chronology of the events leading to the present-day configuration. This might be achieved only if a field-based approach, addressed to geological and geomorphological mapping, is integrated with the analysis of whatever morphometric indexes and remote measurements.
- The Holocene Apennine tectonic stages are witnessed by the co-evolution of regional and local hydrographic networks. The major Alpine-draining rivers (lower plain terrace) entrench and undergo systematic diversions at the Alps-Apennines interference zone, while the streams sourced from the intra-basin hill, to the South, deepen, diverge and are tilted across fault-blocks.
- The studied palimpsest landscape mirrors the migration of compressional-extensional structural domains of the advancing Apennines front across the Po Plain. The Late Quaternary coevolution of the intra-basin highs, formed on the two opposite thrust belts, indicates the basin-scale response to their structural interference. Holocene ongoing thrusting along a deeper sole-thrust is coherent with the seismic framework of the Central-Northern Po Plain. Buttressing along the interference zone is responsible for late, exceeding uplift rates which promoted passive deformation and latest collapse of the southernmost reliefs.

Acknowledgments

We thank Dr. Christoph Grützner and an anonymous Reviewer for their accurate reviews, which helped to improve the manuscript. This work was supported by funds to RB [grant-RV_ATT_COM16RBERS_M].

References

Alessio, G., Alfonsi, L., Brunori, C.A., Burrato, P., Casula, G., Cinti, F.R., Civico, R., Colini, L., Cucci, L., De Martini, P.M., Falcucci, E., Galadini, F., Gaudiosi, G., Gori, S., Mariucci, M.T., Montone, P., Moro, M., Nappi, R., Nardi, A., Nave, R., Pantosti, D., Patera, A., Pesci, A., Pezzo, G., Pignone, M., Pinzi, S., Pucci, S., Salvi, S., Tolomei, C., Vannoli, P., Venuti, A., Villani, F., 2013. Liquefaction phenomena associated with the Emilia earthquake sequence of May-June 2012 (Northern Italy). Nat. Hazards Earth Syst. Sci. 13, 935–947. https://doi.org/10.5194/nhess-13-935-2013

Arca, S., Beretta, G. Pietro, 1985. Prima sintesi geodetico-geologica sui movimenti verticali del suolo nell'Italia Settentrionale. Boll. di Geod. e Sci. Affin. 2. Istituto Geografico Militare, Firenze, IT.

Ariati, L., Cotta Ramusino, S., Peloso, L.G., 1988. La struttura del Colle di San Colombano al Lambro: riflessi idrogeologici e caratteristiche chimiche della falda freatica. In: Casati, P. (Ed.), Acque Sotterranee Di Lombardia. Dipartimento Scienze della terra e CNR - Centro di Studio per la stratigrafia e petrografia delle Alpi Centrali, Milano, pp. 97–115.

Baio, M., Bersezio, R., Bini, A., 2004. Assetto geologico della successione Quaternaria nel sottosuolo tra Melegnano e Piacenza. Il Quaternario 17 (2/1), 355 -359.

Benedetti, L.C., Tapponnier, P., Gaudemer, Y., Manighetti, I., 2003. Geomorphic evidence for an emergent active thrust along the edge of the Po Plain: the Broni-Stradella fault. J. Geophys. Res. 108, 2238. https://doi.org/10.1029/2001JB001546

Bennett, R.A., Serpelloni, E., Hreinsdóttir, S., Brandon, M.T., Buble, G., Basic, T., Casale, G., Cavaliere, A., Anzidei, M., Marjonovic, M., Minelli, G., Molli, G., Montanari, A., 2012. Syn-convergent extension observed using the RETREAT GPS network, northern Apennines, Italy. J. Geophys. Res. Solid Earth 117. https://doi.org/10.1029/2011JB008744

Bersezio, R., 1986. Studio fotogeologico e geofisico per la ricostruzione dell'andamento degli antichi alvei: prima ricostruzione dei paleoalvei della Pianura tra Adda e Ticino, in: Studi Idrogeologici Sulla Pianura Padana. CLUP, Milano, pp. 3.1-3.25.

Bersezio, R., Pavia, F., Baio, M., Bini, A., Felletti, F., Rodondi, C., 2004. Aquifer architecture of the Quaternary alluvial succession of the Southern Lambro Basin (Lombardy - Italy). Ital. J. Quat. Sci. 17, 361–378.

Bertotti, G., Capozzi, R., Picotti, V., 1997. Extension controls Quaternary tectonics, geomorphology and sedimentation of the N-Apennines foothills and adjacent Po Plain (Italy). Tectonophysics 282, 291–301.

Bigi, G., Cosentino, D., Parotto, M., Sartori, D., Scandone, P., 1990. Structural model of Italy. Progett. Final. Geodin. CNR.

Bini, A., Baio, M., Pavia, F., 2015. Analisi di una sezione geologica tracciata tra Adda e Mella, al margine tra alta e bassa pianura. Geol. Insubrica 11 (1)

Bini, A., Baio, M., Violanti, D., Martinetto, E., 2016. Nuovi dati da sondaggi provenienti dai dintorni di San Colombano al Lambro e dalla Pianura Padana a Est di Milano: analisi litostratigrafica, composizionale e micropaleontologica. Geol. Insubrica 12.

Bloom, A.L., 2002. Teaching about relict, no-analog landscapes. Geomorphology 47, 303–311. https://doi.org/10.1016/S0169-555X(02)00094-6

Boccaletti, M., Corti, G., Martelli, L., 2011. Recent and active tectonics of the external zone of the Northern Apennines (Italy). Int. J. Earth Sci. 100, 1331–1348. https://doi.org/10.1007/s00531-010-0545-y

Boni, A., 1967. Note illustrative della Carta Geologica d'Italia. F.°59, Pavia. Servizio Geologico d'Italia, Nuova Tecnica Grafica, Roma, IT.

Bonini, M., 2013. Fluid seepage variability across the external Northern Apennines (Italy): Structural controls with seismotectonic and geodynamic implications. Tectonophysics 590, 151–174. https://doi.org/10.1016/j.tecto.2013.01.020

Bonini, L., Toscani, G., Seno, S., 2014. Three-dimensional segmentation and different rupture behavior during the 2012 Emilia seismic sequence (Northern Italy). Tectonophysics 630, 33–42. https://doi.org/10.1016/j.tecto.2014.05.006

Boschi, E., Guidoboni, E., Ferrari, G., Mariotti, D., Valensise, G., Gasperini, P., 2000. Catalogue of Strong Italian Earthquakes, 461 b.C to 1997. Ann. Geophys. 49, 609–868.

Bresciani, I., Perotti, C.R., 2014. An active deformation structure in the Po Plain (N Italy): the Romanengo anticline. Tectonics 33, 2059–2076. https://doi.org/10.1002/2013TC003422

Bull, W.B., 2007. Tectonic Geomorphology of Mountain: A New Approach to Paleoseismology. Blackwell Publishing, Oxford, UK. https://doi.org/10.1002/gj.1222

Bull, W.B., Mc Fadden, L.M., 1977. Tectonic geomorphology north and south of the Garlock Fault, California. J. Geomorphol. 1, 15–32.

Burbank, D., Anderson, R.S., 2013. Tectonic geomorphology, 2nd ed. ed. Wiley-Blackwell.

Burrato, P., Ciucci, F., Valensise, G., 2003. An inventory of river anomalies in the Po Plain , Northern Italy: evidence for active blind thrust faulting. Ann. Geophys. 46, 865–882.

Butler, R.W.H., 1987. Thrust sequences. Journal of the Geological Society 144, 619-634. https://doi.org/10.1144/gsjgs.144.4.0619

Capozzi, R., Picotti, V., 2002. Fluid migration and origin of a mud volcano in the Northern Apennines (Italy): The role of deeply rooted normal faults. Terra Nov. 14, 363–370. https://doi.org/10.1046/j.1365-3121.2002.00430.xCapozzi, R., Picotti, V., 2010. Spontaneous fluid emissions in the Northern Apennines: geochemistry, structures and implications for the petroleum system. Geol. Soc. London, Spec. Publ. 348, 115–135. https://doi.org/10.1144/SP348.7

Capozzi, R, Menato, V., Rabbi, E., 1994. Manifestazioni superficiali di fluidi ed evoluzione tettonica recente del margine appenninico Emiliano-Romagnolo: Indagine preliminare. Atti Ticinensi di Sci. della Terra 1, 247–254.

Carafa, M.M.C., Barba, S., 2013. The stress field in Europe: Optimal orientations with confidence limits. Geophys. J. Int. 193, 531–548. https://doi.org/10.1093/gji/ggt024

Carminati, E., Martinelli, G., Severi, P., 2003. Influence of glacial cycles and tectonics on natural subsidence in the Po Plain (Northern Italy): Insights from 14 C ages. Geochemistry, Geophys. Geosystems 4.

https://doi.org/10.1029/2002GC000481

Castiglioni, G.B., Pellegrini, G.B., 2001. Note illustrative della Carta Geomorfologica della Pianura Padana. Suppl. di Geogr. Fis. e Din. Quat. - vol. IV. Comitato Glaciologico Italiano, Torino, IT

Chiarini, E., D'Orefice, M., Graciotti, R., 2008. Le unità stratigrafiche di riferimento nella rappresentazione cartografica dei depositi Plio-Quaternari continentali nel progetto CARG - esempi: Arco Alpino, Pianura Padana e Sardegna. Alp. Mediterr. Quat. 21, 51–56.

Chiarle, M., Martinelli, G., Nanni, T., Patrizi, G., Venturini, L., Zuppi, G., 1991. Salt waters, brines and geologic structure of the Apennines front (Northern Italy), in: Isotope Techniques in Water Resources Development. IAEA, STI/PUB/875, Vienna, pp. 691–694.

Conti, A., Turpin, L., Polino, R., Mattei, M., Zuppi, G.M., 2001. The relationship between evolution of fluid chemistry and the style of brittle deformation: Examples from the Northern Apennines (Italy). Tectonophysics 330, 103–117. https://doi.org/10.1016/S0040-1951(00)00224-9

Conti, S., Artoni, A., Piola, G., 2007. Seep-carbonates in a thrust-related anticline at the leading edge of an orogenic wedge: The case of the middle-late Miocene Salsomaggiore Ridge (Northern Apennines, Italy). Sediment. Geol. 199, 233–251. https://doi.org/10.1016/j.sedgeo.2007.01.022

Cox, R.T., 1994. Analysis of drainage-basin symmetry as a rapid technique to identify areas of possible Quaternary tilt-block tectonics: an example from the Mississippi Embayment. Geol. Soc. Am. Bull. 106, 571–581.

Desio, A., 1965. I rilievi isolati della Pianura Lombarda ed i movimenti tettonici del Quaternario. Rend. dell'Istituto Lomb. di Sci. e Lett. A, 881–894.

Devoti, R., Esposito, A., Pietrantonio, G., Pisani, A.R., Riguzzi, F., 2011. Evidence of large scale deformation patterns from GPS data in the Italian subduction boundary. Earth Planet. Sci. Lett. 311, 230–241. https://doi.org/10.1016/j.epsl.2011.09.034

Delcaillau, B., 2001. Geomorphic response to growing fault-related folds: example from the foothills of central Taiwan. Geodinamica Acta 14, 265-287Delcaillau, B., Deffontaines, B., Floissac, L., Angelier, J., Deramond, J., Souquet, P., Chu, H.T., Lee, J.F., 1998. Morphotectonic evidence from lateral propagation of an active frontal fold; Pakuashan anticline, foothills of Taiwan. Geomorphology 24, 263–290

Delcaillau, B., Carozza J.M., Laville, E., 2006. Recent fold growth and drainage development: The Janauri and Chandigarh anticlines in the Siwalik foothills, northwest India Geomorphology 76, 241 –256. doi:10.1016/j.geomorph.2005.11.005

Di Manna, P., Guerrieri, L., Piccardi, L., Vittori, E., Castaldini, D., Berlusconi, A., Bonadeo, L., Comerci, V., Ferrario, F., Gambillara, R., Livio, F., Lucarini, M., Michetti, A.M., 2012. Ground effects induced by the 2012 seismic sequence in Emilia: Implications for seismic hazard assessment in the Po Plain. Ann. Geophys. 55, 697–703. https://doi.org/10.4401/ag-6143

DISS Working Group, 2018. Database of Individual Seismogenic Sources (DISS), Version 3.2.1: A compilation of potential sources for earthquakes larger than M 5.5 in Italy and surrounding areas. http://diss.rm.ingv.it/diss/, Istituto Nazionale di Geofisica e Vulcanologia; doi:10.6092/INGV.IT-DISS3.2.1

Doglioni, C., 1993. Some remarks on the origin of foredeeps. Tectonophysics 228, 1-20.

Dunne, W.M., Ferrill, D.A., 1988. Blind thrust sytems. Geology 16 (1), 33-36. https://doi.org/10.1130/0091-7613(1988)016<0033:BTS>2.3.CO;2

El Hamdouni, R., Irigaray, C., Fernández, T., Chacón, J., Keller, E.A., 2008. Assessment of relative active tectonics,

southwest border of the Sierra Nevada (southern Spain). Geomorphology 96, 150–173. https://doi.org/10.1016/j.geomorph.2007.08.004

Fantoni, R., Bersezio, R., Forcella, F., 2004. Alpine structure and deformation chronology at the Southern Alps-Po Plain border in Lombardy. Boll. della Soc. Geol. Ital. 123, 463–476.

Farolfi, G., Bianchini, S., Casagli, N., 2019. Integration of GNSS and Satellite InSAR Data: Derivation of Fine-Scale Vertical Surface Motion Maps of Po Plain, Northern Apennines, and Southern Alps, Italy. IEEE Trans. Geosci. Remote Sens. 57, 319–328. https://doi.org/10.1109/TGRS.2018.2854371

Fiorani Gallotta, P.L., 1921. Fauna fossile dei colli di San Colombano al Lambro. Arch. Stor. per la città e i Comuni del Circondario e della Diocesi di Lodi, Anno XL 2.

Frigerio, C., Bonadeo, L., Zerboni, A., Livio, F., Ferrario, M.F., Fioraso, G., Irace, A., Brunamonte, F., Michetti, A.M., 2017. First evidence for Late Pleistocene to Holocene earthquake surface faulting in the Eastern Monferrato Arc (Northern Italy): Geology, pedostratigraphy and structural study of the Pecetto di Valenza site. Quat. Int. 451, 143–164. https://doi.org/10.1016/j.quaint.2016.12.022

Ghielmi, M., Minervini, M., Nini, C., Rogledi, S., Rossi, M., 2013. Late Miocene–Middle Pleistocene sequences in the Po Plain – Northern Adriatic Sea (Italy): The stratigraphic record of modification phases affecting a complex foreland basin. Mar. Pet. Geol. 42, 50–81. https://doi.org/10.1016/j.marpetgeo.2012.11.007

Goswami, T.K., Bezbaruah, D., Mukherjee, S., Sarmah, S.K., Jabeed, S., 2018. Structures and morphotectonic evolution of the frontal fold–thrust belt, Kameng river section, Arunachal Himalaya, India. J. Earth Syst. Sci. 127 (88), 1-11. https://doi.org/10.1007/s12040-018-0984-6

Grützner, C., Walker, R. T., Abdrakhmatov, K. E., Mukambaev, A.,Elliott, A. J., Elliott, J. R. , 2017. Active tectonics around Almaty and along the Zailisky Alatau range front. Tectonics 36, 2192–2226. https://doi.org/10.1002/2017TC004657

Grützner, C., Campbell, G., Walker, R. T., Jackson, J., Mackenzie, D.,Abdrakhmatov, K., Mukambayev, A., 2019. Shortening accommodated by thrust and strike-slip faults in the Ili Basin, northern Tien Shan. Tectonics 38, 2255–2274. https://doi.org/10.1029/2018TC005459

Guidoboni, E., Ferrari, G., Mariotti, D., Comastri, G., Tarabusi, G., Valensise, G., 2007. CFTI4Med, Catalogue of Strong Earthquakes in Italy (461 B.C.-1997) and Mediterranean Area (760 B.C.-1500), Available from http://storing.ingv.it/cfti4med/.

Holbrook, J., Schumm, S.A., 1999. Geomorphic and sedimentary response of rivers to tectonic deformation: A brief review and critique of a tool for recognizing subtle epeirogenic deformation in modern and ancient settings. Tectonophysics 305, 287–306. https://doi.org/10.1016/S0040-1951(99)00011-6

Howard, A.D., 1967. Drainage Analysis in Geologic Interpretation: A Summation. Am. Assoc. Pet. Geol. Bull. 51, 2246–2259.

Keller, E.A., Pinter, N., 2002. Active Tectonics - Earthquakes, Uplift, and Landscape, Second Ed. ed. Prentice-Hall.

Keller, E.A., Gurrola, L., Tierney, T.E., 1999. Geomorphic criteria to determine direction of lateral propagation of reverse faulting and folding. Geology 27 (6), 515–518

Knuepfer, P.L., 1989. Implications of the characteristics of end-points of historical surface fault ruptures for the nature of fault segmentation. U.S. Geol. Surv. Open-File Rep. 89, 193–228.

Leopold, L.B., Tricard, J., 1967. Field methods for the study of slope and fluvial processes. Rev. Geomorph. Dyn 4.

Leopold, L.B., Wolman, M.G., 1957. River Channel Patterns: Braided, Meandering and Straight. United States

Government Printing Office, Washington.

Liotta, D., Cernobori, L., Nicolicl, R., 1998. Restricted rifting and its coexistence with compressional structures: Results from the CROP 3 traverse (northern Apennines, Italy). Terra Nov. 10, 16–20. https://doi.org/10.1046/j.1365-3121.1998.00157.x

Livani, M., Scrocca, D., Arecco, P., Doglioni, C., 2018. Structural and Stratigraphic Control on Salient and Recess Development Along a Thrust Belt Front: The Northern Apennines (Po Plain, Italy). J. Geophys. Res. Solid Earth 123, 4360–4387. https://doi.org/10.1002/2017JB015235

Livio, F.A., Berlusconi, A., Zerboni, A., Trombino, L., Sileo, G., Michetti, A.M., Rodnight, H., Spotl, C., 2014. Progressive offset and surface deformation along a seismogenic blind thrust in the Po Plain foredeep (Southern Alps, Northern Italy). J. Geophys. Res. Solid Earth 1482–1497. https://doi.org/10.1002/2013JB010193.Received

Maesano, F.E., D'Ambrogi, C., Burrato, P., Toscani, G., 2015. Slip-rates of blind thrusts in slow deforming areas: Examples from the Po Plain (Italy). Tectonophysics 643, 8–25. https://doi.org/10.1016/j.tecto.2014.12.007

Maestrelli, D., Benvenuti, M., Bonini, M., Carnicelli, S., Piccardi, L., Sani, F., 2018. The structural hinge of a chain-foreland basin: Quaternary activity of the Pede-Apennine Thrust front (Northern Italy). Tectonophysics 723, 117–135. https://doi.org/10.1016/j.tecto.2017.12.006

Malik, J.N., Shah, A.A., Naik, P.S., Sahoo, S, Okumura, K., Patra, N. R., 2014. Active fault study along foothill zone of Kumaun Sub-Himalaya: influence on landscape shaping and drainage evolution. Current Science 106 (2), 229-236

Mayer, L., Menichetti, M., Nesci, O., Savelli, D., 2003. Morphotectonic approach to the drainage analysis in the North Marche region, central Italy Quaternary International 101–102, 157–167

Marchetti, M., 2002. Environmental changes in the central Po Plain (northern Italy) due to fluvial modifications and anthropogenic activities. Geomorphology 44, 361-373. https://doi.org/10.1016/S0169-555X(01)00183-0

McCalpin, J., 2009. Paleoseismology. Academic Press, Inc., San Diego.

McClay, K., R., (Ed.) 1992. Thrust Tectonics. 447 pp., Springer. https://doi.org/10.1007/978-94-011-3066-0.

Michetti, A.M., Giardina, F., Livio, F., Mueller, K., Serva, L., Sileo, G., Vittori, E., Devoti, R., Riguzzi, F., Carcano, C., Rogledi, S., Bonadeo, L., Brunamonte, F., Fioraso, G., 2012. Active compressional tectonics, quaternary capable faults, and the seismic landscape of the po plain (northern Italy). Ann. Geophys. 55, 969–1001. https://doi.org/10.4401/ag-5462

Molli, G., Carlini, M., Vescovi, P., Artoni, A., Balsamo, F., Camurri, F., Clemenzi, L., Storti, F., Torelli, L., 2018. Neogene 3-D Structural Architecture of The North-West Apennines: The Role of the Low-Angle Normal Faults and Basement Thrusts. Tectonics 37, 2165–2196. https://doi.org/10.1029/2018TC005057

Montenat, C., Barrier, P., D'Estevou, P., 1991. Some aspects of the recent tectonics in the Strait of Messina, Italy. Tectonophysics 194, 203–215.

Montenat, C., Barrier, P., D'Estevou, P., Hibsch, C., 2007. Seismites: An attempt at critical analysis and classification. Sediment. Geol. 196, 5–30. https://doi.org/10.1016/j.sedgeo.2006.08.004

Montone, P., Mariucci, M.T., Pierdominici, S., 2012. The Italian present-day stress map. Geophys. J. Int. 189, 705–716. https://doi.org/10.1111/j.1365-246X.2012.05391.x

Morley, C.K., 1986. A classification of thrust fronts. AAPG Bulletin 70 (1), 12-25.

Morley, C.K., 1988. Out-of-sequence thrusts. Tectonics 7 (3), 539-561. https://doi.org/10.1029/TC007i003p00539

Mouthereau, F., Lacombe, O., Deffontaines, B., Angelier, J., Chu, H. T., Lee, C.T., 1999. Quaternary transfer faulting and belt front deformation at Pakuashan (western Taiwan) Tectonics 18 (2), 215-230.

NACSN (North American Commission on Stratigraphic Nomenclature), 2005. North American Stratigraphic Code. Am. Assoc. Pet. Geol. Bull. 89, 1547–1591. https://doi.org/10.1306/07050504129

Oppo, D., Viola, I., Capozzi, R., 2017. Fluid sources and stable isotope signatures in authigenic carbonates from the Northern Apennines, Italy. Mar. Pet. Geol. 86, 606–619. https://doi.org/10.1016/j.marpetgeo.2017.06.016

Ori, G.G., 1993. Continental depositional systems of the Po plain (Northern Italy). Sediment. Geol. 83, 1-14.

Panzeri, L., Zembo, I., Bersezio, R., Martini, M., 2011. Calibration of OSL data: mismatch between stratigraphy and OSL chronology pf sediments from the Po Plain. Quat. 24, 114–116.

Pearce, S.A., Pazzaglia, F.J., Eppes, M. C., 2004 Ephemeral stream response to growing folds. GSA Bulletin 116(9/10), 1223–1239. doi: 10.1130/B25386.1;

Pedrera, A., Pérez-PeñaJ.V., Galindo-Zaldívar, J., Azañón, J.M., Azor, A., 2009. Testing the sensitivity of geomorphic indices in areas of low-rate active folding (eastern Betic Cordillera, Spain) Geomorphology 105, 218–231 doi:10.1016/j.geomorph.2008.09.026

Pellegrini, G.B., Vercesi, P.L., 1995. Considerazioni morfoneotettoniche sulla zona a sud del Po tra Voghera (PV) e Sarmato (PC). Atti Ticinensi di Sci. della Terra 38, 95–118.

Pellegrini, L., Boni, P., Carton, A., 2003. Hydrographic evolution in relation to neotectonics aided by data processing and assessment: some examples from the Northern Apennines (Italy). Quat. Int. 101–102, 211–217. https://doi.org/10.1016/S1040-6182(02)00103-9

Picotti, V., Pazzaglia, F.J., 2008. A new active tectonic model for the construction of the Northern Apennines mountain front near Bologna (Italy). J. Geophys. Res. Solid Earth 113, 1–24. https://doi.org/10.1029/2007JB005307

Pieri, M., Groppi, G., 1981. Subsurface geological structure of the Po plain, Italy, in: Progetto Finalizzato Geodinamica. CNR, Progetto Finalizzato Geodinamica, p. 13.

Piovene G., 1888. Cronaca dei terremoti a Vicenza, Annali dell'Ufficio centrale di Meteorologia e Geodinamica, IV, 13, 238-1887.

Pizzi, A., Galadini, F., 2009. Pre-existing cross-structures and active fault segmentation in the northern-central Apennines (Italy). Tectonophysics 476, 304–319. https://doi.org/10.1016/j.tecto.2009.03.018

Pondrelli, S., 2002. European-Mediterranean Regional Centroid-Moment Tensors Catalog (RCMT). https://doi.org/10.13127/rcmt/euromed

Pondrelli, S., Salimbeni, S., Morelli, A., Ekström, G., Postpischl, L., Vannucci, G., Boschi, E., 2011. European-Mediterranean Regional Centroid Moment Tensor catalog: Solutions for 2005-2008. Phys. Earth Planet. Inter. 185, 74–81. https://doi.org/10.1016/j.pepi.2011.01.007

Ponza, A., Pazzaglia, F. J., Picotti, V., 2010. Thrust-fold activity at the mountain front of the Northern Apennines (Italy) from quantitative landscape analysis. Geomorphology 123, 211–231 doi:10.1016/j.geomorph.2010.06.008

Postpischl D., 1985. Catalogo dei terremoti italiani dall'anno 1000 al 1980. Progetto Finalizzato Geodinamica. "Quaderni de «La Ricerca Scientifica»", n.114, v.2B.

Ramírez-Herrera, M.T., 1998. Geomorphic assessment of active tectonics in the acambay graben, Mexican volcanic belt. Earth Surf. Process. Landforms 23, 317–332. https://doi.org/10.1002/(SICI)1096-

9837(199804)23:4<317::AID-ESP845>3.0.CO;2-V

Ramsay, J.G., Huber, M.I., 1987. The techniques of modern structural geology Vol. 2, Folds and fractures. Elsevier Science Ltd.

Regione Lombardia, Eni Divisione Agip, 2001. Geologia degli acquiferi padani della Regione Lombardia. S.EL.CA., Firenze, Italy. https://doi.org/10.1017/CBO9781107415324.004

Ricci Lucchi, F. , 1986. Oligocene to Recent foreland basins of northern Apennines. In: Foreland Basins (Eds P Allen and P. Homewood), IAS Special Publication 8, 105-139.

Rovida, A., Locati, M., Camassi, R., Lolli, B., Gasperini, P. (Eds.), 2016. CPTI15, the 2015 version of the Parametric Catalogue of Italian Earthquakes. Istituto Nazionale di Geofisica e Vulcanologia. https://doi.org/10.6092/INGV.IT-CPTI15

Scardia, G., De Franco, R., Muttoni, G., Rogledi, S., Caielli, G., Carcano, C., Sciunnach, D., Piccin, A., 2012. Stratigraphic evidence of a Middle Pleistocene climate-driven flexural uplift in the Alps. Tectonics 31, TC6004.. https://doi.org/10.1029/2012TC003108

Schumm, S.A., Dumont, J.F., Holbrook, J.M., 2002. Active tectonics and alluvial rivers. Cambridge University Press.

Silva, P.G., Goy, J.L., Zazo, C., Bardají, T., 2003. Fault generated mountain fronts in Southeast Spain: geomorphologic assessment of tectonic and earthquake activity. Geomorphology 250, 203–226.

Singh, T., 2008. Tectonic implications of geomorphometric characterization of watersheds using spatial correlation Mohand Ridge, NW Himalaya, India. Zeitschrift für Geomorphologie 52, 4, 489–502.

Singh, T., Jain, V., 2009. Tectonic constraints on watershed development on frontal ridges: Mohand Ridge, NW Himalaya, India. Geomorphology 106, 231–241. doi:10.1016/j.geomorph.2008.11.001

Spagnolo, M., Pazzaglia, F.J., 2005. Testing the geological influences on the evolution of river profiles: A case from the northern Apennines (Italy). Geogr. Fis. e Din. Quat. 28, 103–113.

Strahler, A.., 1957. Quantitative analysis of watershed morphology. Trans. Am. Geophys. Union 38, 913–920.

Toscani, G., Seno, S., Fantoni, R., Rogledi, S., 2006. Geometry and timing of deformation inside a structural arc : the case of the western Emilian folds (Northern Apennine front , Italy). Boll. della Soc. Geol. Ital. 125, 59–65.

Toscani, G., Bonini, L., Ahmad, M.I., Di Bucci, D., Di Giulio, A., Seno, S., Galuppo, C., 2014. Opposite verging chains sharing the same foreland: Kinematics and interactions through analogue models (Central Po Plain, Italy). Tectonophysics 633, 268–282 http://dx.doi.org/10.1016/j.tecto.2014.07.019

Turrini, C., Angeloni, P., Lacombe, O., Ponton, M., Francois, R., 2015. Three-dimensional seismo-tectonics in the Po Valley basin, Northern Italy. Tectonophysics 661, 156–179.

Valensise, G., Vannoli, P., Burrato, P., Fracassi, U., 2020. From Historical Seismology to seismogenic source models, 20 years on: Excerpts from the Italian experience. Tectonophysics 774, 228189. https://doi.org/10.1016/j.tecto.2019.228189

Vannoli, P., Burrato, P., Valensise, G., 2015. The Seismotectonics of the Po Plain (Northern Italy): Tectonic Diversity in a Blind Faulting Domain. Pure Appl. Geophys. 172, 1105–1142. https://doi.org/10.1007/s00024-014-0873-0

Vannucci, G., Gasperini, P., 2004. The new release of the database of earthquake mechanisms of the Mediterranean area (EMMA Version 2). Ann. Geophys. 47, 307–317. https://doi.org/10.4401/ag-3277

Veggiani, A., 1982. Variazioni climatiche e dissesti idrogeologici dell'Alto Medioevo in Lombardia e la rifondazione di Lodi. Sibrium 16, 199–208.

Whittaker, A.C., Attal, M., Cowie, P.A., Tucker, G.E., Roberts, G., 2008. Decoding temporal and spatial patterns of

fault uplift using transient river long profiles. Geomorphology 100, 506–526. https://doi.org/10.1016/j.geomorph.2008.01.018

Yin, A., 2006. Cenozoic tectonic evolution of the Himalayan orogen as constrained by along-strike variation of structural geometry, exhumation history, and foreland sedimentation. Earth-Science Reviews 76, 1 –131. doi:10.1016/j.earscirev.2005.05.004

Zámolyi, A., Székely, B., Draganits, E., Timár, G., 2010. Neotectonic control on river sinuosity at the western margin of the Little Hungarian Plain. Geomorphology 122, 231–243. https://doi.org/10.1016/j.geomorph.2009.06.028

Zanchi, A., Deaddis, M., De Amicis, M., Marchetti, M., Ravazzi, C., Vezzoli, G., 2019. Holocene deformed succession of Montodine (Cremona, Italy): evidence of recent tectonic activity?, in: Carmina, B., Petti, F.M., Innamorati, G., Fascio, L. (Eds.), Congresso SIMP-SGI-SOGEI. Società Geologica Italiana, Parma, p. 499. https://doi.org/10.3301/ABSGI.2019.05

Ziegler P., A. and Fraefel, M., 2009. Response of drainage systems to Neogene evolution of the Jura fold-thrust belt and Upper rhine Graben. swiss J. Geosci. 102, 57–75. DOI 10.1007/s00015-009-1306-4

Zuffetti, C., 2019. Characterization and modelling of complex geological architectures: The Quaternary fill of the Po Basin at the Po Plain-Apennines border (Lombardy, Italy), 246 pp., PhD Thesis. Università degli Studi di Milano. Milano.

Zuffetti, C., Bersezio, R., Contini, D., Petrizzo, M.R., 2018a. Geology of the San Colombano hill, a Quaternary isolated tectonic relief in the Po Plain of Lombardy (Northern Italy). J. Maps 14, 199–211. https://doi.org/10.1080/17445647.2018.1443166

Zuffetti, C., Trombino, L., Zembo, I., Bersezio, R., 2018b. Soil evolution and origin of landscape in a late Quaternary tectonically mobile setting: the Po Plain-Northern Apennines border in Lombardy (Italy). Catena 171, 376–397. https://doi.org/10.1016/j.catena.2018.07.026

Zuffetti, C., Bersezio, R., Trombino, L., 2018c. Significance of the morphological and stratigraphic surfaces in the Quaternary Po Plain : the San Colombano tectonic relief (Lombardy, Italy). Alp. Mediterr. Quat. 31, 257–260.

Websites

AGEA - Agenzia per le Erogazioni in Agricoltura (Agency for Agricultural Supply). 2012. https://www.agea.gov.it

Geoportale Regione Lombardia (Geoportal of Lombardy Region). www.geoportale.regione.lombardia.it

Seismic catalog of INGV - Istituto Nazionale di Geofisica e Vulcanologia (National Institute of Geophysics and Volcanology) http://cnt.rm.ingv.it

FIGURE CAPTIONS

Fig. 1 – A) Location map of the study area in the structural and seismic framework of the Po Plain (Northern Italy). The study area (black frame) hosts the southernmost of a set of intra-basin isolated reliefs. Buried S-Alpine structures simplified from Fantoni et al. (2004). Buried N-Apennines structures from Bigi et al. (1990). Location of historical earthquakes after INGV (http://cnt.rm.ingv.it); Rovida et al. (2016). Earthquakes focal mechanisms from EMMA (Earthquake Mechanisms of the Mediterranean Area; Vannucci and Gasperini, 2004) catalog and RCMT (European-Mediterranean Regional Centroid Moment Tensor; Pondrelli et al, 2002) catalog of INGV. CCS: Capriano del Colle Structure, CPPS: Central Po Plain Structures, RS: Romanengo structure, SCS: San Colombano hill Structure, CZS: Casalpusterlengo-Zorlesco Structure, CZTF: Casalpusterlengo-Zorlesco Transfer Fault, BSF: Broni-Stradella Fault, FHS: Foothill Structures. B) Stratigraphic and landscape units of the San Colombano hill study area (location in panel A). F1-F3: interpreted map-scale fault systems, orientations: N160E (F1); N060E (F2); N110E (F3). Modified after Zuffetti et al. (2018a).

Fig. 2– Morphological features and measured meso-structures of the San Colombano hill area, mapped on the 5 m DTM of Lombardy region (www.geoportale.regione.lombardia.it).

Fig. 3 – The hydrography of the San Colombano hill. A) Drainage network and sub-basin divides. Table: selected morphometric features of the numbered basins. S_0–S_{16}: geomorphic segments (see text for discussion); Bs: basin shape; AF: asymmetry factor. Bold numbers highlight narrow-elongated basins (high Bs values); underlined numbers refer to the most asymmetric basins. B) Selected longitudinal stream profiles across the central-eastern hill (labels as in panel A). Knickpoints (white dots) are distributed at comparable elevations in adjacent streams and locate on triangular facets (compare to Figure 2). C) S-ward deepening asymmetric valley of basin 26.

Fig. 4 – The hydrography of the plain adjacent to the San Colombano hill. A) DSM of the study area highlighting the main directions of (paleo-) river traces compared to the hillslopes orientations. S_0–S_{16}: geomorphic segments as in Fig. 3. Black frames: location of panels B-C-D. B) The western study area: anomalous N-ward dip of the plain adjacent to the hill (compare white-black triangles). C) Terraced plain N of the central-eastern hill. 1 to 3: interpreted chronology of the mapped scarps. D) South of the hill: N110E-trending ridges (black double lines) separate elongated incisions. 1 to 3: interpreted chronology of paleo-river shifting towards SW.

Fig. 5 – The San Colombano hillslopes and hilltop. A) Detail of triangular and trapezoidal facets bounding the northern flank of the hill, observed from the North-West and West (left- and right-hand side panel, respectively). B) Hillslope morphology along the southern side of the hill, observed from the South-East. Valley diversions (curved arrows) are common at the straight hill boundaries. Google Earth views, vertical exaggeration 3x. S_0-S_{11up}: reference faceted hill front segments presented in the box at the right-hand side. J: mountain front sinuosity index; Fd: degree of facet development (x: low, xx: high); Fh: facet height in meters.

Fig. 6 – Perspective views of the topography of the San Colombano hill, highlighting the relationships between the main morphostructural elements and the interpreted fault systems F1, F2, F3.

Fig. 7 - The palimpsest landscape of the San Colombano hill area. Colour scale: interpreted relative chronology of the landforms of the hill and adjacent terraced plain. Arrows: direction of the paleo-drainage. Line marks (*): the colour of the oblique bars

refers to chronology of reworking of the plain terraces (in solid-fill colour) following the general colour scale of the map. Letters A-E relate each landform to the stage of morpho-tectonic evolution presented in Fig. 8. Description of the landscape units in Section 4. Left-hand corner: location of the study area in the structural framework of the Po foreland basin (legend as in Fig.1).

Fig. 8 – Late Quaternary evolution of the San Colombano hill landscape, and its relationship with the interpreted evolution of the Northern Apennines deformation front. The study area is framed by the black rectangle. Upper corner on the left-hand side of each panel: kinematic interpretation of the major active structural trends. Labels of the Apennines structures as in Fig. 1. Encircled numbers: landforms mapped in Fig. 7 whose origin derives from the here-presented increments.

Table 1 – Slip rates and uplift rate ranges along the South Alpine and Northern Apennines thrusts in the Central Po foreland basin. DSR/RSR: dip parallel/rake parallel slip rates.

ID (Fig. 1-A)	Fault system (Fig. 1-A)	Age interval	Slip rate [mm/yr]	Slip rate type	Uplift rate [mm/yr]	Authors
a	CCS	0.8 My-present	0.47	DSR	0.22	Livio et al. (2009)
b	RS	Late Pleistocene-present			0.12	Bresciani and Perotti (2014)
c	CPPS	1.8 My-present	0.19	DSR		Maesano et al. (2015)
d	Outer Emilia Arcs	1.8 My-present	0.51	DSR		Maesano et al. (2015)
	Outer Emilia Arcs	1.8 My-present	1.5	RSR		Boccaletti et al. (2011)
e	BSF	Late Pleistocene-present			0.3	Benedetti et al. (2003)
f	FHS	0.8 My-present	0.5	DSR	0.1-0.3	Wilson et al. (2009)
g	Inner Emilia Arcs	0.8 My-present	0.22	DSR		Maesano et al. (2015)
h1	Inner Emilia Arcs	0.8 My-present	0.26	DSR		Maesano et al. (2015)
h2	Inner Emilia Arcs	0.8 My-present	0.3	DSR		Maesano et al. (2015)

Table 2 – The geomorphological dataset and the related GIS elements surveyed and analysed in this work.

Geomorphological datum	GIS element	Geomorphological datum	GIS element
Topographic elevation point	point FC	Geomorphological boundary	polyline FC
Dip-direction of the topographic surface	point FC	Fault	polyline FC
Sub-horizontal agrarian parcel	point FC	Longitudinal profile	polyline FC
Hump; hollow	point FC	Trace of topographic profile	polyline FC
Windgap	point FC	Drainage basin	polygon FC
Saddle	point FC	Planation surface	polygon FC
Back-tilted surface	point FC	Ranked geomorphological unit	polygon FC
Downstream end of hanging valley	point FC	Topographic basemaps	raster dataset
Ranked escarpment (natural; anthropic)	polyline FC	Digital Terrain Model	raster dataset
Rectilinear/cruvilinear tract of the stream network	polyline FC	Digital Surface Model	raster dataset
Drainage divide	polyline FC	Slope and aspect map	raster dataset
Trace of abandoned hydrography	polyline FC	Longitudinal profile graph	raster dataset
Landslide rim	polyline FC	Topographic profile graph	raster dataset
Ridge (tectonic; fluvial)	polyline FC		

FC: GIS Feature Class

Declaration of interests

☒ The authors declare that they have no known competing financial interests or personal relationships that could have appeared to influence the work reported in this paper.

☐The authors declare the following financial interests/personal relationships which may be considered as potential competing interests:

Graphical abstract

HIGHLIGHTS

1. Palimpsest landscapes mirror polyphase tectonic evolution of foreland basins
2. Effects of locked, blind thrust-and-fold belts on surface processes and landforms
3. Field-based case-history on morphotectonics of the Quaternary Po Foreland Basin
4. Late Pleistocene growth, segmentation and collapse of intrabasinal highs
5. Neotectonics and seismicity control the river network of basins and highs